CHALMERS

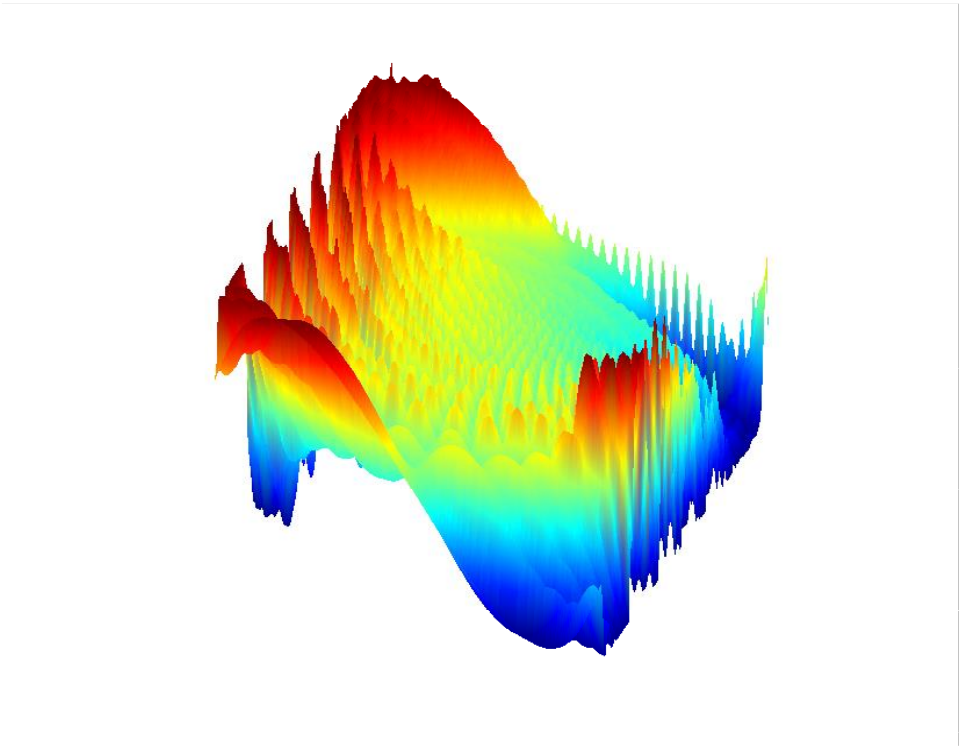

Detection of stationary lobe in AESA radar

Detecting loss of lobe movement and estimating the lobe direction through observations of near-field microwave radiation

Master of Science Thesis in Systems, control and mechatronics

KIM VIGGEDAL

Department of Signals and systems
Division of control enginnering
CHALMERS UNIVERSITY OF TECHNOLOGY
Gothenburg, Sweden, 2013
Report No. EX067/2013

Abstract

The goal of this thesis has been to implement a system which can detect stationarity of the main lobe in an AESA (Active Electronically Scanned Antennas) antenna. This system is to be used at the test rig during system integration and verification of the radar system, hence the implemented system is not allowed to trust any information from the radar system. Detection of a stationary main lobe must be completely independent of the radar system functionality. Secondary to the goal of implementing the system capable of detecting stationarity of the main lobe was the aim to investigate further possibilities to track the lobe direction based on measurements similar to those in the implemented system.

The project can be considered as composed of three main parts:

- The first 3 chapters of the report describe the initial part where a literature study was made parallel to simulations. This part provided an overview of the problem and the methods available to solve it.
- Chapter 4 describes the second part where algorithms both for detection of stationary main lobe and for tracking of the lobe direction were investigated and compared.
- In chapter 5 the third part of the project is described; practical aspects of the implementation of the detection system, and some discussion about results acheived with the implemented system.

The method of choice for measurements and data acquisition is an extremely small and simple sensor array of two receiving AEs (Antenna Elements). In section 4 the observability of the lobe direction through this system is discussed and it is shown how stationarity of the main lobe is detectable through a slow and simple average power sensor.
Further discussion in section 4 is mainly focused on the applicability of Kalman filters. It is suggested that a PLL (Phase Locked Loop) filter based on Kalman filtering could improve the performance of a similar sensor array with faster and more flexible signal processing.

The simple solution using an average power sensor was implemented at the system rig and initial testing suggests it should work well. The system is to be used at the system rig after final verification.

For future work on the topic it could be interesting to investigate how Kalman filter based PLL filtering would perform compared to conventional ML DOA (Maximum Likelihood Direction Of Arrival) estimation of the lobe direction.
It could also be interesting to implement the Kalman filter based design in a software defined radio platform such as GNU Radio on a USRP (Universal Software Radio Peripheral) and compare theory with reality.

Acknowledgements

This work has been carried out at Saab EDS (Electronic Defence Systems) and the Department of Signals and Systems at Chalmers University of Technology.

I would like to thank the many coworkers at Saab who have been so very enthusiastic and supportive throughout this work. Especially I want to thank my supervisor Rikard Bergman for his dedicated guidance and mentoring. I also want to thank my supervisor Professor Claes Breitholtz for some much appreciated and helpful feedback.

Abbreviations, acronyms and technical terms

AA	Antenna Array
AE	Antenna elements
AESA	Active Electronically Scanned Antenna
Boresight	Antenna aperture normal
DARE	Discrete time Algebraic Riccati Equation
DOA	Direction Of Arrival
DOU	DOrsal Unit, ERIEYE radar antenna
FPGA	Field Programmable Gate Array
Jitter	Signal deviation from true periodicity
Lobe	Local maximum in the radiation pattern of an antenna
MLDOA	Maximum Likelihood DOA
Observer	Control theory concept, state estimator
PLL	Phase locked loop
RF	Radio Frequency
SISO	Single Input Single Output
USRP	Universal Software Radio Peripheral, hardware platform
PVA model	Position-Velocity-Acceleration model

Contents

1. Background

At Saab EDS in Gothenburg several radar systems are developed and produced, one of which is the airborne surveillance radar ERIEYE. Testing of new radar systems includes live operation from the test facilities at Kallebäck.
The ERIEYE system being designed for long range airborne surveillance operates at relatively high power levels. The high output power has caused concerns regarding the electric field strength in close proximity to the test rig. Simulations have shown that microwave power levels will become unacceptably high, in parts of the area close to the test rig, if the lobe is fixed in specific directions for prolonged times.

Of course, any risk to personal safety when testing the system is unacceptable. Thus there is a need for a solution which can guarantee that the radar is never transmitting in a fixed direction.
The purpose of the work described in this thesis was to implement a system, separate from the radar, to supervise the lobe movement and shut off radar transmission if the lobe stops moving.

Figure 1: SAAB 2000 equipped with ERIEYE system.

Since the radar antenna is of AESA type it doesn't rotate like traditional radar antennas. The antenna is instead a large array of smaller AEs, each with a controlled phase.
The phase of each AE is controlled such that interference between AEs is constructive only in a narrow direction from the antenna, causing the total antenna gain to increase in this direction. By controlling the phase of each AE it is possible to control the antenna directionality almost arbitrarily, at very high speeds.
Though, since there is no mechanical movement involved in the radar scanning it can't be measured by angular sensors in servos. For the monitoring of the scanning to be independent of the system it is monitoring, estimates must be made through measurements of the nearby electric field.

This work aims to develop the above described system for supervisory control of the radar system. The thesis includes a review of the typical electric fields for this type of antenna and determining a practical way to measure physical quantities for estimating the sweep over time. Equipment needed for these measurements is also to be selected. Furthermore an algorithm for detecting dangerous sweep patterns is to be obtained and implemented in software.
Measurements to verify suggested detection methods were performed during initial radar tests with limited transmission and the complete system is to be verified and demonstrated before the radar antenna is tested for full transmission capabilities.

1.1. Active electronically scanned antennas

AESA are built up by large arrays of small antennas. They are commonly used in radar applications for their ability to dynamically change the shape and direction of the radiation pattern, making them much faster and more versatile than mechanically scanned radar systems.
AESA radar achieves this by controlling the phase of the AEs, thus controlling the diffraction pattern of the array.
The specific radar antenna of interest usually operates by continuously scanning one or several areas. The areas can have different shapes and sizes and are defined by the operator. The areas can also have different priorities, demanding different rates of information updating, causing the radar to jump between areas in an order which will best satisfy priorities.
The scanning speed can also be set to a number of predefined rates. The operator can change the scanning speed at any time.
If any moving objects are detected, a track is initiated to record the position and speed of the moving object over time.
Furthermore, for some modes of operation; if any tracks are acquired these will have requirements on the rates at which information about the track is updated. If the current scanning pattern takes too long to revisit the last known position of a track, the scanning will be interrupted and the lobe will make an instantaneous jump to the estimated target position in order to require new information about position, speed and course.

This dynamic behavior is very demanding for any supervision system as smooth scanning patterns can’t be assumed and sampling should ideally be performed at high GHz frequencies. If the radar had only been able to scan, not making any discrete jumps to update tracks, Kalman filtering or some other model based filtering technique could have been used to filter out measurement noise. However, from the perspective of the supervision system, the lobe direction is changed independently of previous directions –making Kalman filtering of lobe directions estimates pointless. The actual probability density of the lobe direction is constant rather than Gaussian.

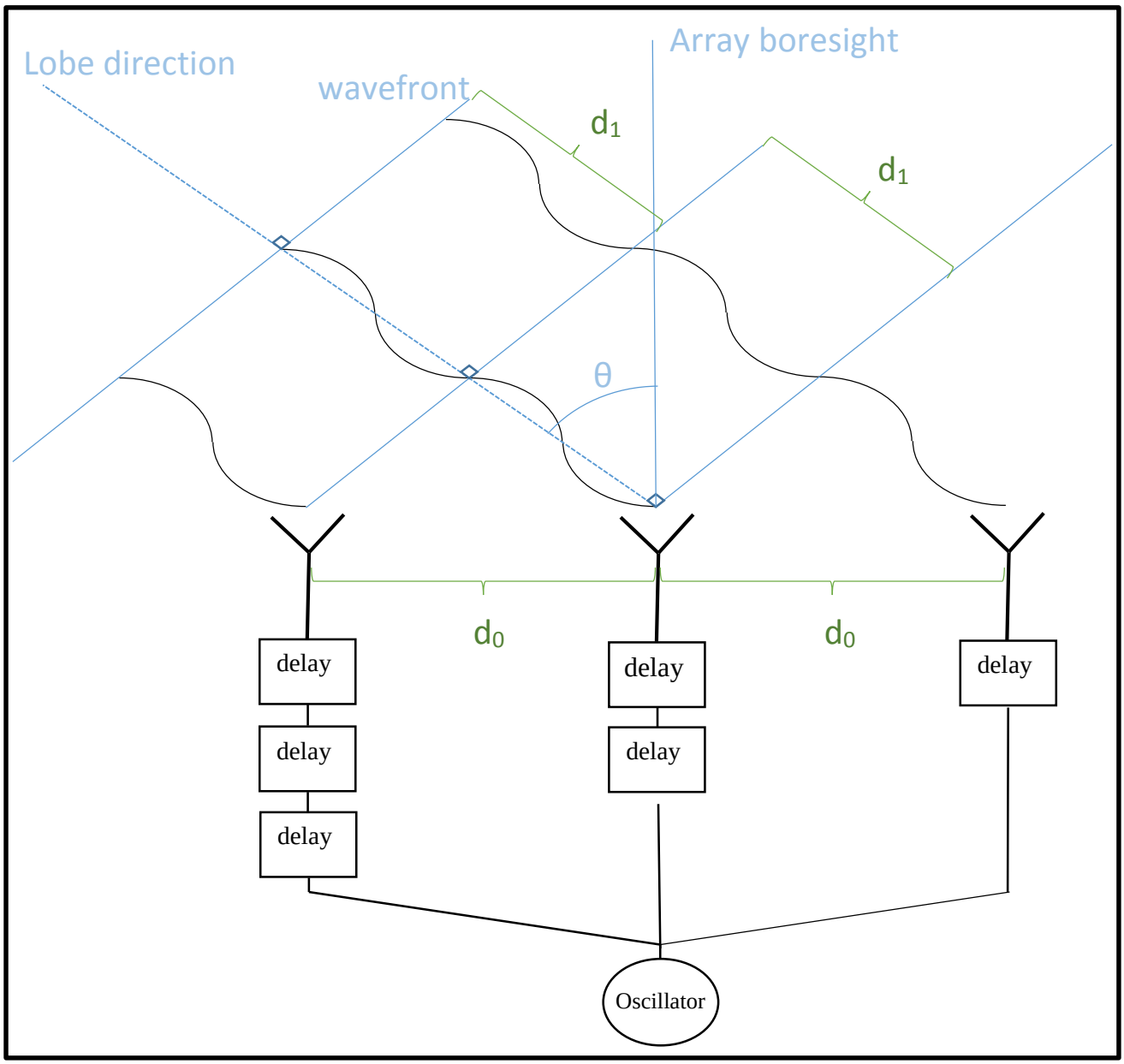

Figure 2: Description of lobe direction control and definition of the lobe direction θ.

The lobe direction of the antenna is described in terms of the angle between the wave front normal and the antenna normal, this angle is equal to the angle between the far field wave front and the aperture. The relation between lobe direction and controlled phase shift is:

$$\theta = \sin^{-1}\left(\varphi \frac{\lambda}{2\pi d_0}\right) \qquad (1)$$

Where:
$\lambda \sim wavelength\ of\ the\ radar\ signal$
$\theta \sim lobe\ direction$
$\varphi \sim control\ signal, determining\ the\ phase\ shift\ at\ antenna\ elements$
$d_0 \sim distance\ between\ consecutive\ antenna\ elemen$
$d_1 \sim distance\ between\ wavefronts\ \ from\ consecutive\ antenna\ elements$

1.2. Problem definitions and solution requirements

The primary problem addressed in this thesis is to implement a system for automatic detection of a stationary lobe. The implemented system will hereafter be referred to as the supervision system.
Secondary to this problem is an investigation of how the supervision system could be improved to allow accurate estimation of lobe direction by use of an observer based on Kalman filtering.

The requirements on the supervision system are in short;

- It should detect loss of lobe movement and shut down transmission power if the lobe is fixed in any direction.
- Loss of lobe movement must be detected fast enough so that the electric field caused by the radar is never at risk of breaching the safety regulations.

Even though the antenna is divided into several sections of several AEs the supervision system should consider it as a whole.
No distinction between partial antenna failure and complete antenna failure is required, i.e. the AA is assumed to always behave like one large unit, where either all sections of the antenna work to produce a moving main lobe or no section of it does so.

Work with microwave producing equipment is regulated by a document from the Swedish authority Arbetsmiljöverket [1].

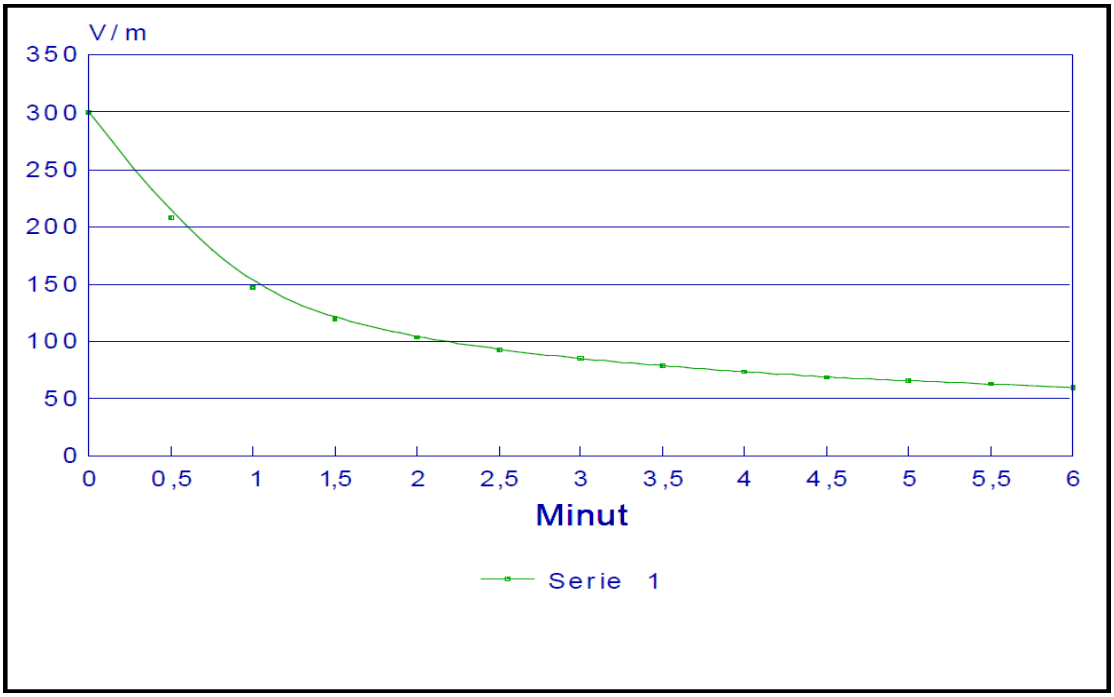

Figure 3: The y-axis corresponds to average electric field strength and the x-axis corresponds to the time of exposure to the electric field. The green trace describes the time limit for exposure at different varying average strengths of the electric field.

Prescribed limits for transmission of electromagnetic waves are expressed as time limits varying with the average strength of the electric and magnetic fields generated.
Figure 3 describes the time limit for varying average electric field strengths if the maximum level of average power is to be kept equivalent to the power exposure of the maximum allowed average electric field strength according to [1].
The plot in figure 3 is what has been used to determine how time limits should be chosen to satisfy requirements.

Previous simulations, presented in [2], have investigated the electric field in the vicinity of the antenna in terms of regulations in [1]. The simulations investigated a set of possible transmission scenarios where the antenna was tilted to 0˚, 5˚ and 10˚ elevation. For each case the electric field strength along all possible transmission directions was calculated given fixed transmission in the respective direction.
Regulations state that the allowed time of exposure for 300 V/m average electric field strength is 1 second, while an average electric field strength of 60 V/m is allowed for 6 minutes. Lower electric field strengths than 60 V/m are not subject to time limits.

Direct measurements of the electric field in all of the affected area is obviously not possible. Thus, Saab must rely on simulations of transmission scenarios to predict risks of breaching regulations regarding the electric fields emitted. Being forced to rely on simulations, Saab has decided that transmissions at the system rig should be kept below half the given limits, in order to keep margins for unmodelled reflections.

The simulations of the 0˚ tilt scenario predict that the electric field strengths in the area can exceed 150 V/m during extreme errors. There are currently no plans to allow this scenario. The scenario of 5˚ tilt is predicted to result in a maximum of 135 V/m for fixed direction transmissions. This is the extreme of possible errors for planned transmission scenarios.

To keep margins for unmodelled reflections all simulation results are doubled. Thus the worst case transmission scenario was assumed to generate electric field strengths of 270 V/m. According to the document in [3], the allowed time of exposure to 270 V/m is given by figure 3. This figure suggests a maximum exposure time of approximately 15 seconds. To keep some margin the supervision system should be able to perform detection and cut the transmission within 10 seconds in case of a stationary lobe.

2. Literature study

The field of signal processing techniques aimed at radar applications has developed continuously since the breakthrough of radar technology during the Second World War. Consequently; signal processing in the context of radar technology is a very mature research area with rich literature.
One core problem of radar technology is that of estimating the direction from which an echo arrives at a sensor array, so called Direction Of Arrival-estimation (DOA). It has since long been known that the maximum likelihood-estimator (MLDOA) has very good performance regarding this problem, though MLDOA is also computationally expensive and plenty of research has been done on finding less costly algorithms [4],[5],[6].
Studies have also been performed on optimizing the performance and cost of sensor arrays utilizing different sensor distributions for different specialized cases. Arrays can vary in sensor density and shape depending on the application [5],[7],[8].
The examples referenced here are only a selection from an overwhelmingly large number of papers to give an overview of the research area of radar-applied signal processing.

Even though radar-applied signal processing is a very mature area, with well formalized problem definitions and solutions the author doesn't know of any previous work on the specific problem of this thesis. Estimating the direction of transmission of one sensor array using measurements from a second sensor or sensor array is not quite the same problem as regular DOA estimation. Fortunately this particular problem doesn't appear to be a more complicated problem than DOA estimation.
The reason that this problem has avoided attention before could very well be that there are no obvious reasons to confirm the transmission direction of a sensor array by means of separate equipment in the context of operational radar systems. The most plausible motivation for development of such equipment is probably that of the thesis at hand: A verification tool is required for testing systems in the development phase.
This problem can usually be avoided by planning the test range such that the problem is eliminated rather than solved. For instance the work described in this thesis would not be necessary if the radar system of interest had been tested from a position only a few floors higher up in the building. Mounting the AA at a greater height during tests could increase the distance to the nearby terrain enough to lower microwave power levels in the surrounding area to acceptable levels even in case of faulty transmission.
However, for logistical reasons the radar system will be tested from the current test rig, requiring supervision of the lobe movement.

Even though no previous work on the specific problem of interest has been found, the richness of material regarding AAs and signal processing provided plenty of help. As previously mentioned; modelling and simulation of AAs has been extensively researched and [9] among others have guided the modelling of the AA in this thesis.
Literature on far field and near field models for antennas [9],[10],[11] has provided a basis for choice of hardware and sensor positioning.
Furthermore the extensive research in Phase locked loop filters and Kalman filters [12],[13],[14],[15],[16],[17] and [18] proved very useful for solving a core part of the problem: namely to synchronize estimates of lobe direction with the radar signal to enable estimates of phase shift between the AEs.

3. Simulations

Extensive simulations were performed to investigate the properties of the electric field in the proximity of the antenna. The simulations were aimed at giving an overview of the electric field and how it changes with the distance to the antenna.
It was hoped that this would eventually reveal a way to observe the lobe direction through measurements of the field intensity at one or a few points close to the antenna.

Simulations from previous investigations described the electric field as quite complex, with small variations of the field strength with variations in lobe direction. In the volume where measurements are practically possible to perform the electric field is not lobe shaped, it mostly resembles the shape of Fresnel diffraction through a rectangular aperture.
The simulations performed to investigate the near field of the radiation pattern showed that the entire area directly in front of the antenna surface was excited no matter where the lobe was pointing.

Throughout all simulations of the electric field of the AA, one reference coordinate frame was used. The origin is in the center of the antenna surface; with the z-axis along the boresight, the x-axis along the horizontal axis of the antenna and the y-axis along the vertical axis of the antenna.

Simulations for different measurement points along the antenna surface showed that only on the far sides of the antenna was there possibly a useful relation between lobe direction and intensity of the electric field. To demonstrate this, simulations were performed in which the measurement position was moved along the horizontal axis of the antenna surface, along the vertical axis of the antenna surface and along the diagonal of the antenna surface.

From studying simulation data it was concluded that:

1. Measuring the strength of the electric field at any point in front of the antenna, within a distance of approximately one meter of the antenna surface, could allow detection of lobe movement.
2. Measuring slightly further out from the antenna surface, far out on the sides of the antenna, would give weak measurement signals for small lobe directions with exponentially increasing field strength with increasing angles between lobe direction and antenna boresight.

With these conclusions made, there was an attempt to fine tune the measurement position to a point where electric field strength would be monotonously increasing with increasing angle between lobe direction and antenna bore sight.
No such position could be found, the output was always oscillating, though with low pass filtered measurements (moving average window), something quite usable was achieved.

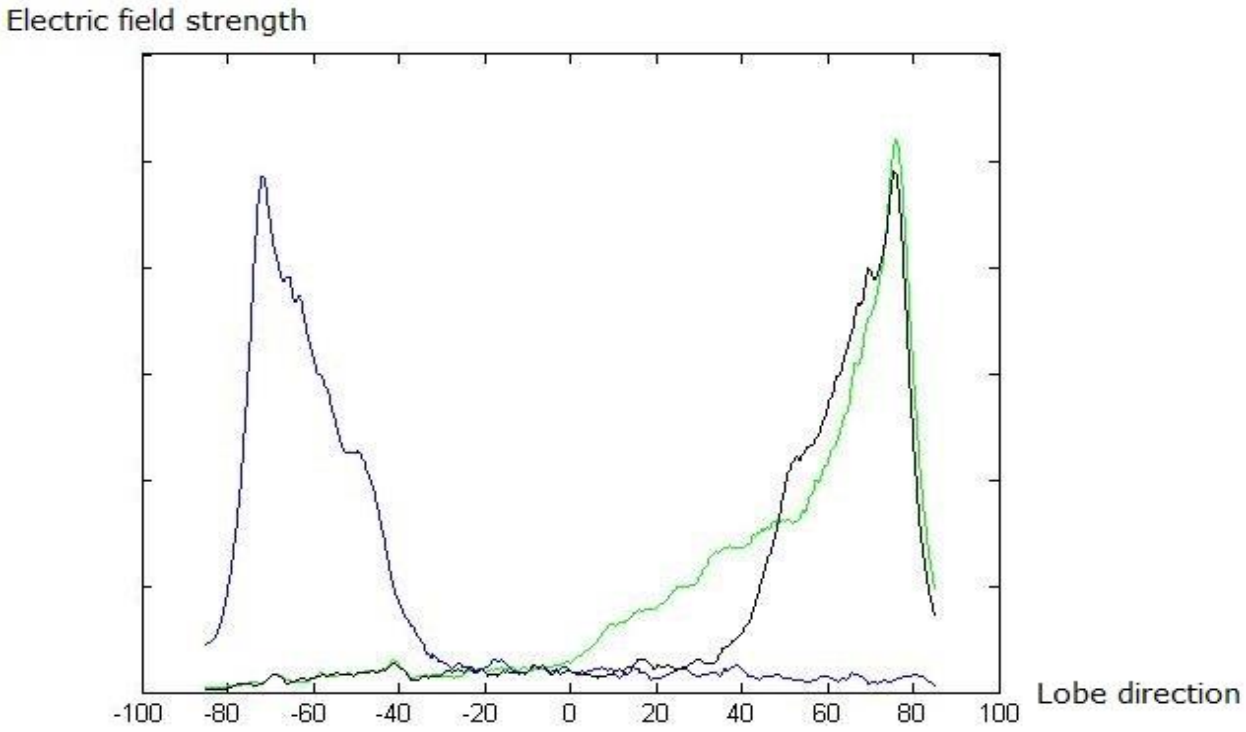

Figure 4: Y-axis ~ electric field strength, X-axis ~ lobe direction (in degrees).
The blue trace describes the output of a sensor far to the left, the black trace describes the output of a sensor far to the right. The green trace describes the output of a sensor on the right side, though somewhat closer to the center of the antenna. All three curves are low pass filtered outputs.

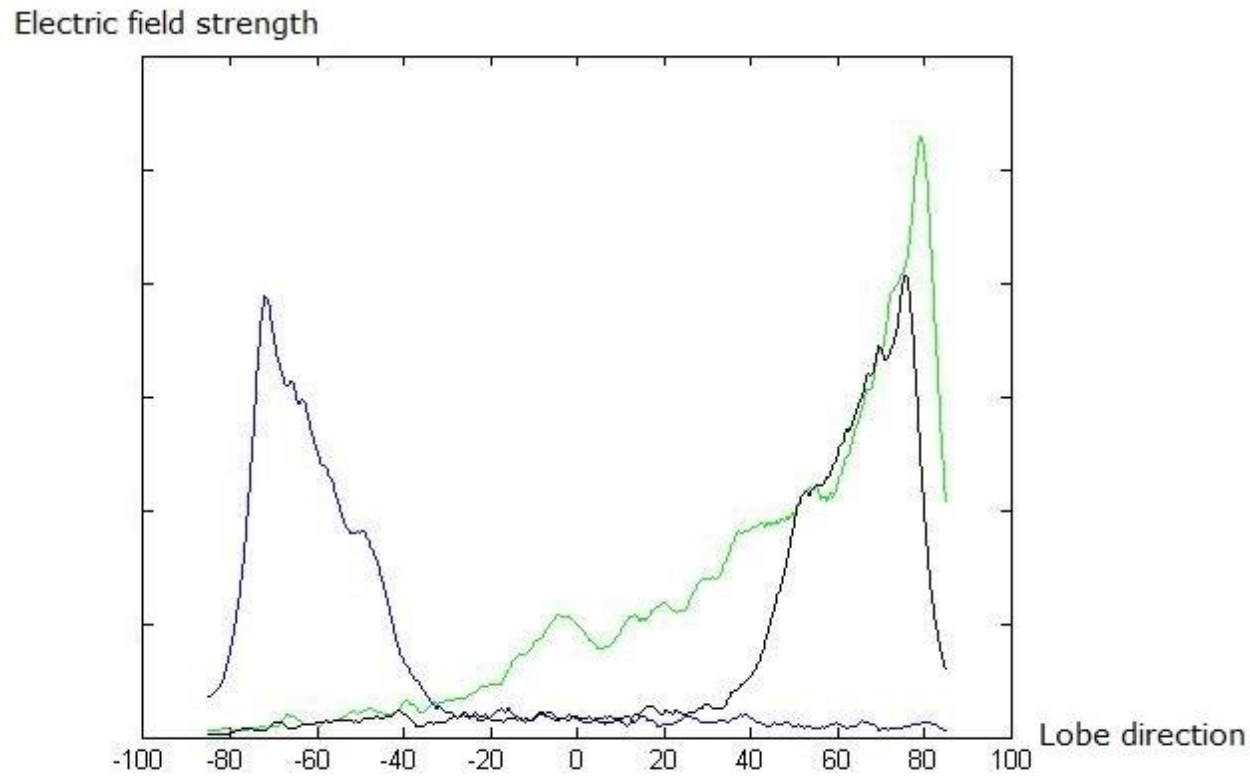

Figure 5: A variation of figure 4 with slightly changed measurement positions for all sensors.

Figure 4 and 5 show the two simulations with sensor positions where the lobe direction could be roughly estimated from the measured intensity of the electric field. These are two of the best cases found when it comes to the range of directions covered with a single sensor and the possibility of explicitly mapping electric field intensities to lobe directions.
Though even these best cases were severely degraded by small variations in sensor position, which is problematic.

As previously mentioned these simulations where aimed at finding a way to easily relate the lobe direction to the intensity of the electric field, or at least a way to detect lobe movement through the same measurements. Detecting lobe movement through measurement of this kind seemed straight forward though for estimating lobe direction these kinds of measurement seemed impractical if at all possible.
The reason for attempting to estimate the lobe direction from the intensity of the electric field was that such a method would allow using a simple, cheap and easily available average power sensor. Though this type of sensor is also quite slow and risked averaging the measurements over a window so long that lobe movement might not be detectable, depending on search area and scan rate.

An alternative approach was considered. The lobe direction is directly related to the phase difference between two consecutive AEs. Tracking the phase of a signal would require much faster sampling than the average power sensor is capable of however, there is a way of enabling estimates of phase difference of the two AEs.
Using two sensors and combining their signals in an analog circuit the interference between the two signals would directly relate the intensity of the combined output to the phase difference between the signals from the two sensors.
The amplitude modulated signal achieved this way would vary with the same speed as the lobe direction, allowing use of the slow but practical average power sensor to track the lobe direction.
The phase oriented approach using double sensors became the method of choice for further investigation.

4. Theory

A detailed description of antenna modelling is outside the scope of this thesis, however a few fundamental concepts will be reviewed. When describing antennas in general it is common to distinguish between far field and near field characteristics. Generally it is the far field characteristics that are important to the application while, for practical reasons, measurements and experimental characterization have to be performed in the near field region.

For the problem of detecting a stationary lobe in an AESA radar, it is impractical to measure in the far field region of the AA. However, when modelling AAs, it is common practice to model the AEs separately as dipole far field patterns and adding them together. This model is valid for regions that can be considered to be in the far field of the smaller AEs and it allows modelling the near field of an AA using only far field modelling techniques.
The AEs in the array of interest are electromagnetically short antennas, thus; assumptions of far field characteristics should be valid at distances more than a couple of wave lengths from the array. In other words the model should be adequate for distances over approximately 0.2 m from the AA.

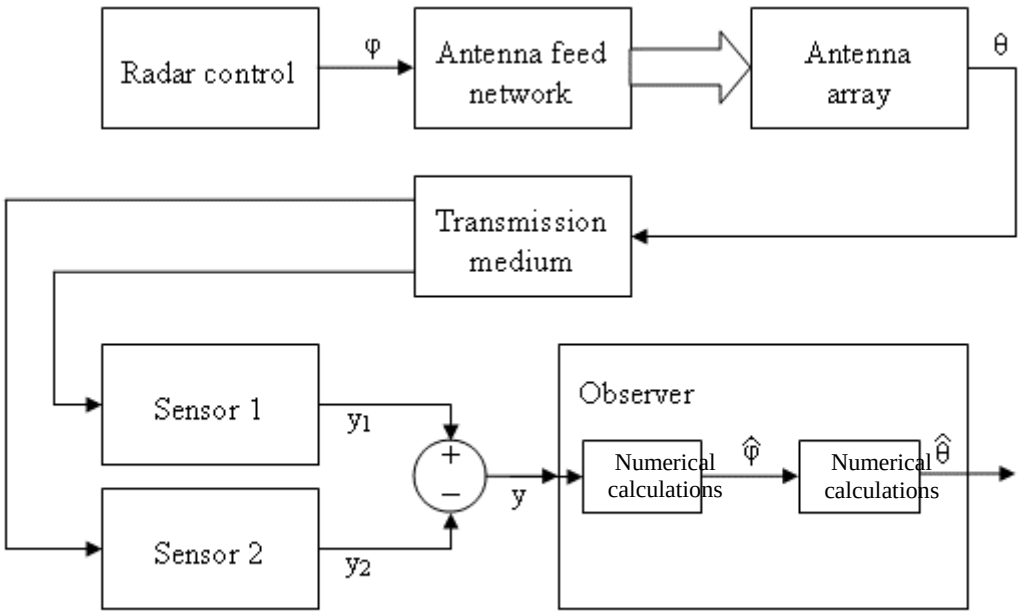

Figure 6: The 3 top process blocks are all part of the radar antenna. Sensor 1 and Sensor 2 register the electric field strengths at two points in the vicinity of the antenna and these two signals are added together. The combined signal y is measured with an average power meter before the observer estimates θ based on the latest measurement.

The following section of the report will derive the output *y(t)*. The task of estimating the lobe direction by following the phase of the output signal *y(t)* has, as will be shown, a unique solution, under assumption of well-known signal paths. Though, as previously mentioned the task is not to estimate the direction of the lobe, only to detect loss of movement of the lobe. Therefore, this method will not be implemented in the final solution, only investigated theoretically.

A stationary lobe would generate a constant *y(t)* whereas a smooth scanning pattern would generate an oscillating output. Non faulty scanning patterns can vary in a seemingly endless number of ways, and are usually not smooth. For the special case of a known scanning pattern, Kalman filters can be used for estimating the lobe direction. Though, as will be more thoroughly discussed in 4.3.1, for the more general case of random lobe direction with constant probability distribution Kalman filters are not well suited.

4.1. Modelling the AESA

When observed through only one receiving antenna; the radar antenna can be seen as a SISO-system, consisting of a set of *N* pulsed oscillators with equal frequencies.
The input of this system is the reference phase τ_θ and the output is the observed sum of pulses y_0.
The phase reference sent to the oscillators can be considered to be the control signal.
Consider the output of the system to be the sum of all states with individual delays corresponding to the distances between the point of observation and the respective AE.

In figure 7 there is an oscillator and a pulse train source, the signals are mixed and fed to each of the *N* AEs. The signal processing performed at each AE is described below:

1. As the sine signal is fed to an AE, it is phase shifted –as a means to control lobe direction. The phase shift is $n \cdot \tau_\theta$ degrees, where *n* is the index of the AE.
2. The phase shifted sine signal is mixed with the pulse train to generate pulsed outputs at the AEs. The pulses are synchronized.
3. As the pulses y_n travel through the transmission medium they are attenuated with constant attenuation a_n and the phase is turned proportionally to the distance travelled through the medium, before they are observed by a sensor.
4. At the sensor, all pulses with their corresponding attenuation and phase are summed together in the output y_0 (as can be seen in figure 7).

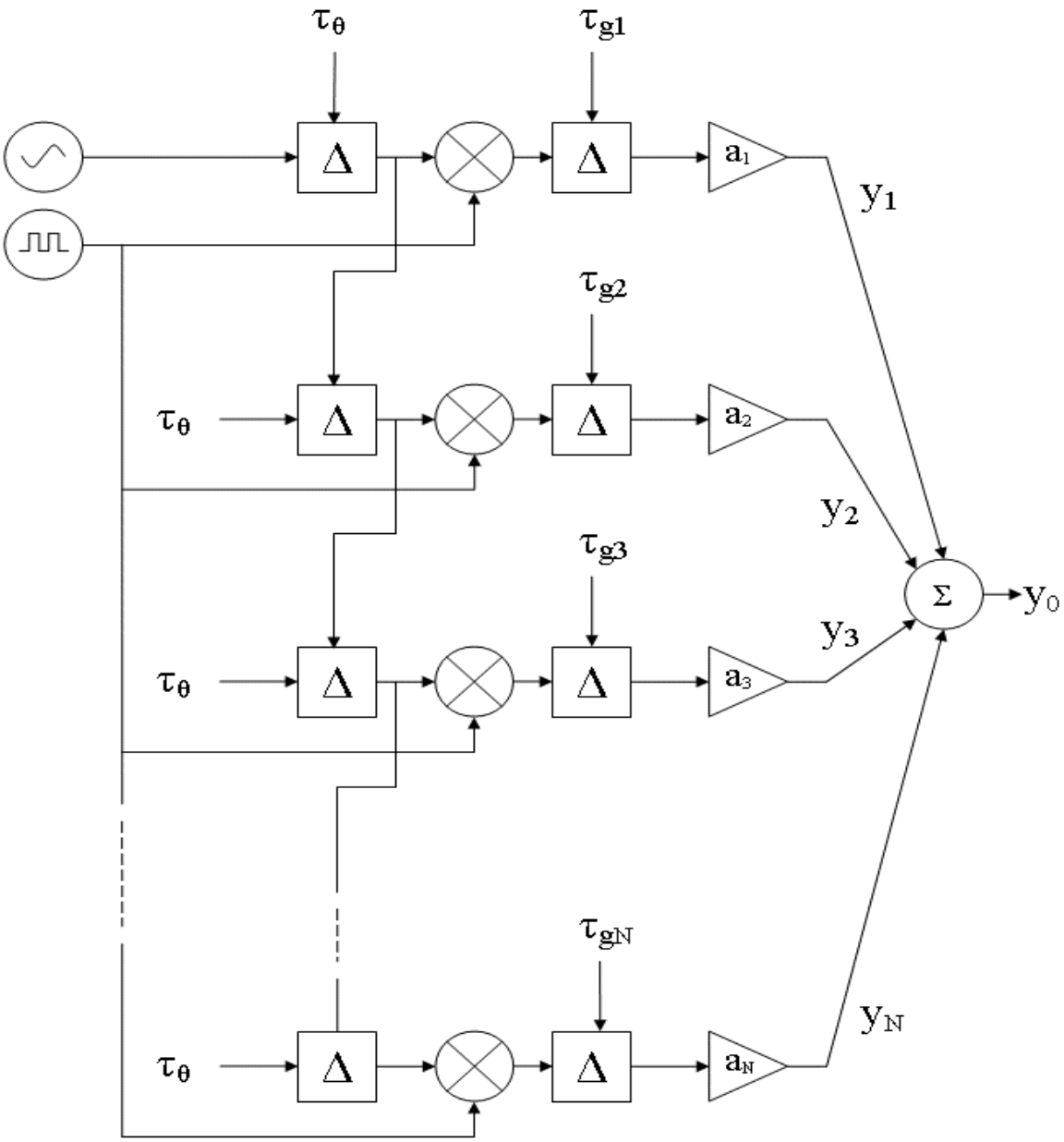

Figure 7: A GHz RF-signal is generated by radar circuits. This RF-signal is feed to each AE, where it is phase shifted and mixed with a pulse signal. The phase shifted and pulsed signal are transmitted through a medium which phase shift the signals further and attenuates them. In the receiver, also called the sensor, all transmitted signals are added together and the result is the output which is later measured with a RF average power meter.

Blocks with delta symbols phase shifts the signal.
Crossed circular symbols are multipliers.
Triangular blocks are amplifiers.

When modelling AAs, it is generally done from the perspective of observing a point source from far away, through the many elements of the AA as in [4]. However for the particular application of this thesis a more unusual problem will be investigated. The problem of interest is a reversed variant where signals originate from the AEs to be observed at a single point some distance from the antenna.

Consider the following system:

$$y(t) = \sum_{n=1}^{N} a_n e^{j(n-1)\varphi} e^{j\delta_n} \mathrm{e}^{j\omega t}$$

Where:

$a_n \in R, is\ the\ constant\ attenuation\ of\ signal\ n\ as\ observed\ through\ y(t),$
$i.e.\ a\ constant\ depending\ on\ the\ sensor\ position.$

$\varphi \in R, is\ the\ phase\ difference\ between\ consecutive\ antenna\ elements, i.e: \varphi = \tau_\theta.$
$i.e.\ a\ constant\ depending\ on\ the\ distribution\ of\ AEs\ position.$

$\delta_n \in R, is\ the\ phase\ shift\ of\ signal\ n\ as\ it\ travels\ from\ its\ source\ to\ the$
$receiver\ y(t), i.e.\ a\ constant\ depending\ on\ the\ sensor\ position.$

$\omega \in R, is\ the\ angular\ speed\ of\ the\ radar\ pulse.$

$N \sim number\ of\ antenna\ elements.$

No analytical solution for φ, given y(t), has been found in this work. However, assuming two sensors $y_1(t)$ and $y_2(t)$ observing the output of the antenna from two different positions it was determined that the phase difference between $y_1(t)$ and $y_2(t)$ could be used to find φ.

Simulations described in 4.2 showed how the phase difference between $y_1(t)$ and $y_2(t)$ is related to φ. These simulations show that optimal observability of φ is achieved when the two sensors are placed at opposite ends of the AA, or both in front of the exact middle of the antenna; depending on which measurement method is chosen.

4.2. Observability of the modelled system

Using the suggested model there are two approaches for implementing the system, both based on placing one sensor at each end of the AA and relating the phase difference between the two outputs to φ.
There is also a third possibility of placing the two sensors just next to each other; this allows for simpler connections between components and could be sufficient for detecting loss of lobe movement.

- Pass both $y_1(t)$ and $y_2(t)$ through one full wave rectifier each, subtract $y_2(t)$ from $y_1(t)$ and measure the resulting signal with an RF average power sensor.
- Pass both $y_1(t)$ and $y_2(t)$ through one full wave rectifier each, then pass each signal through a logarithmic amplifier and finally subtract $y_2(t)$ from $y_1(t)$ and measure with an RF average power sensor.
- Placing the two sensors closer two each other (the same distance apart as is used for the AEs of the ERIEYE antenna)

Both approaches appear to achieve their respective optimal observability when sensors are placed at one end each of the AA.

4.2.1. Implemented system

An average power sensor is to slow to follow the lobe movement accurately, though it is sufficient for detecting loss of lobe movement within a reasonable time limit.
Since full observability of the lobe direction is not necessary, the implemented system is slightly simplified. The full wave rectifiers is left out of the signal processing and as a consequence; the output is oscillating according to the plot in figure 9. The averaging of the output when observed with the power sensor is assumed to smooth out these oscillations.

It is evident from figure 9 that even without the oscillations the signal processing achieves no good observability of the lobe direction without a complementary method to distinguish between negative and positive lobe directions.

The output plotted in figure 9 is the amplitude, i.e. it is not the output given directly by the RF average power sensor though it describes the amplitude of the signal which the sensor measures.

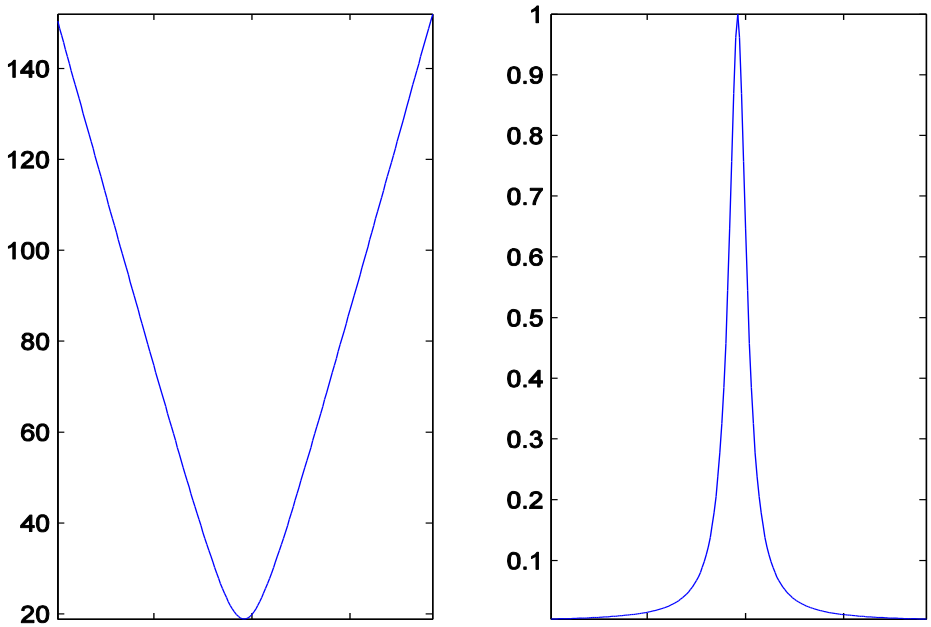

Figure 8: To the left – phase of received signal (in degrees) as a function of the index of the element transmitting the signal.
To the right – normalized plot of power levels of the received signal as a function of the index of the element transmitting the signal.
This simulation assumes synchronized AEs, i.e. a lobe direction along the antenna normal.

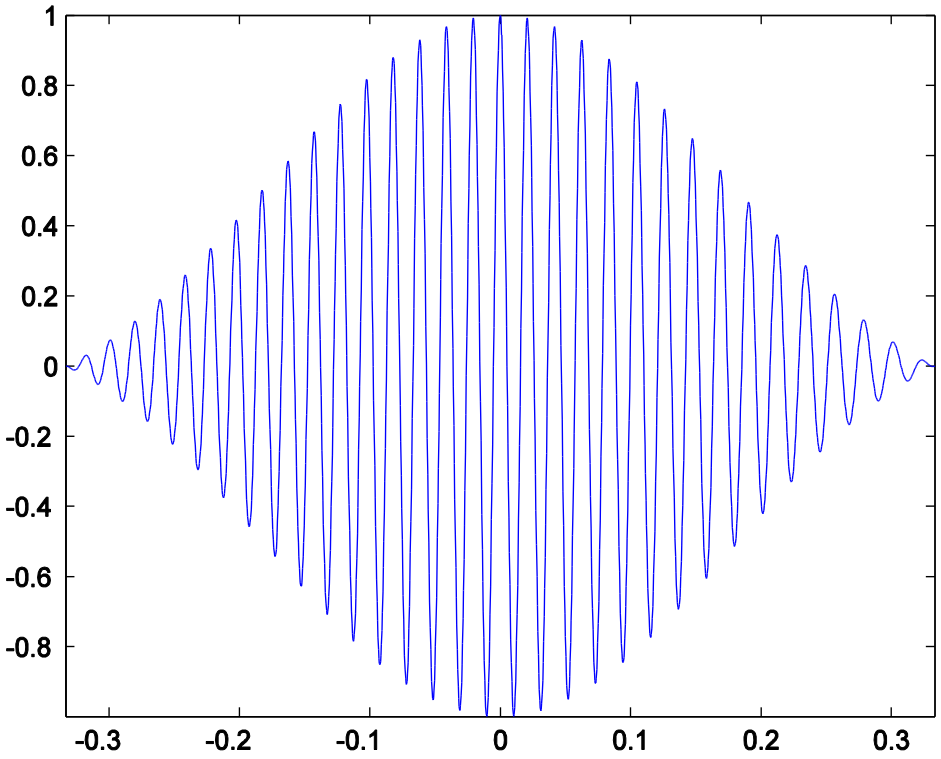

Figure 9: Output amplitude (normalized) as a function of control phase (in π radians). The greatest and smallest control phases in the plot correspond to maximum and minimum lobe steering (-π and π radians from bore sight).
Sensors are positioned 4 AEs apart.

4.2.2. Theoretical observer

Estimates of the lobe direction based on the measurement methods described in the beginning of 4.2 can both provide good observability of the lobe direction. High accuracy and fast tracking is achievable, given fast enough sampling. Though, both methods are very sensitive to the positioning of the sensors.

Figure 10 describes how the mapping from φ to the phase difference between $y_1(t)$ and $y_2(t)$ depend on the sensor positioning. Assume the sensors are positioned right in front of the AA. The axis ranging from 0 to X correspond to half the number of AEs between the two sensors; i.e. a zero means that both sensors are at the exact middle of the antenna and X means that the sensors are positioned at the ends of the AA.

The plots in figure 10 are hard to get a good overview of, therefore the outputs corresponding to the optimum sensor distribution, for each method respectively, are extracted and presented in figures 11 and 12 below.

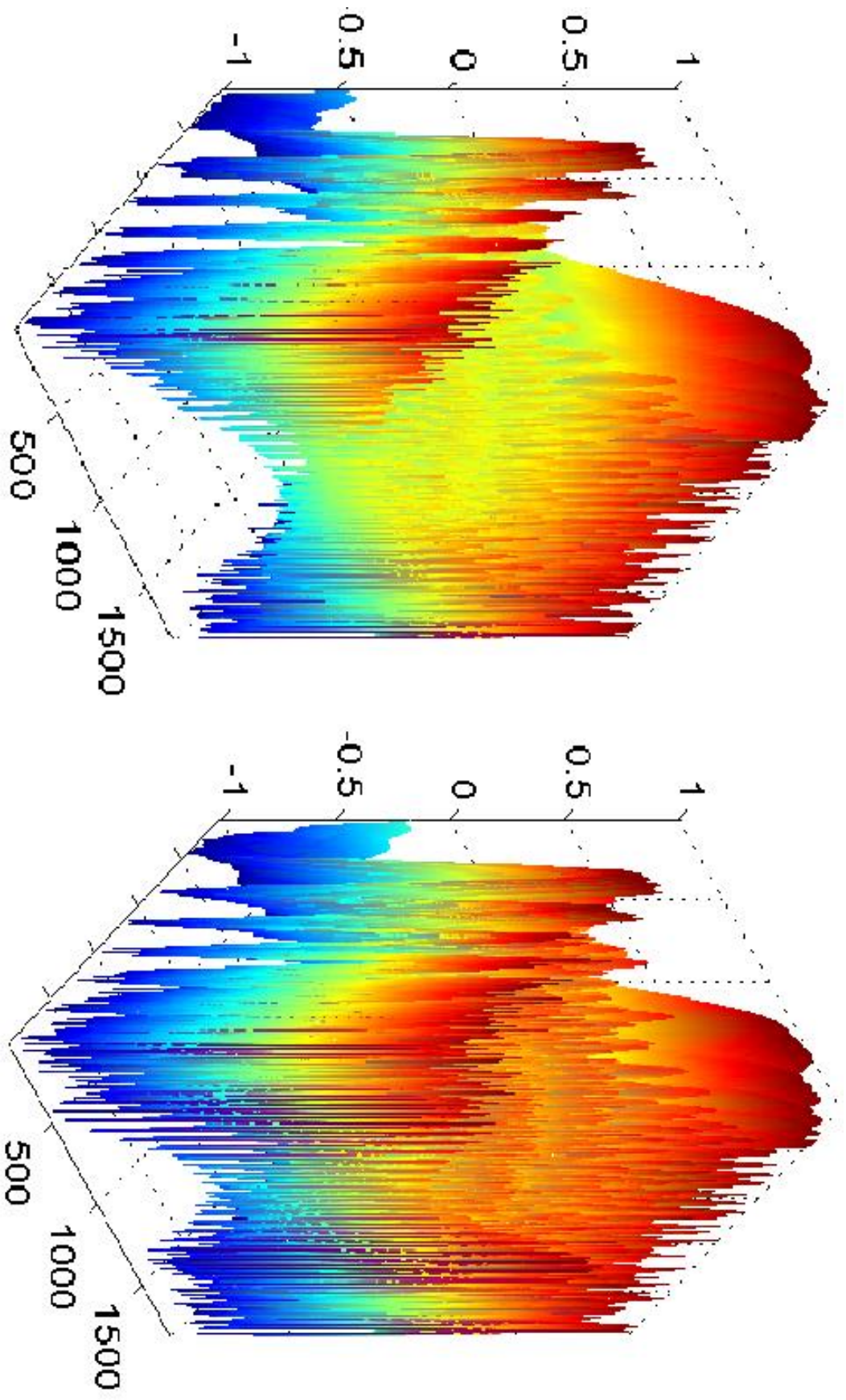

Figure 10: Normalized output as a function of lobe direction and sensor distribution. Lobe directions range from –π to π with 1800 steps in between.
*To the left – signal processing without logarithmic **amplifiers**.*
To the rigth - signal processing with logarithmic amplifiers.

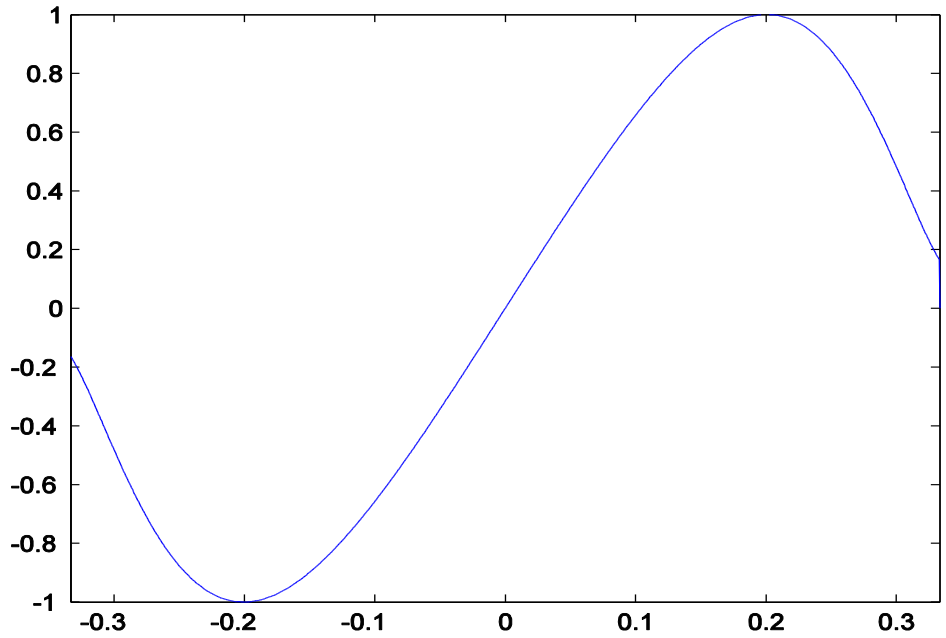

Figure 11: Normalized output when not using optimum sensor distribution but no logarithmic amplifiers.
Y-axis; normalized output.
X-axis: lobe steering (from -π to +π radians)

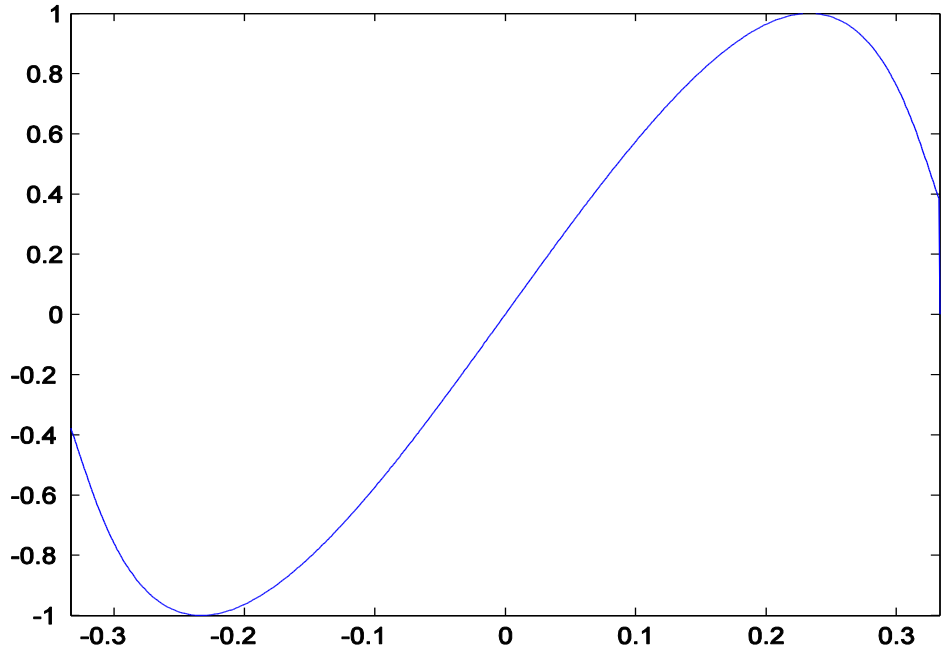

Figure 12: Normalized output when not using optimum sensor distribution and logarithmic amplifiers.
Y-axis; normalized output.
X-axis: lobe steering (from -π to +π radians)

In figures 11 and 12, the lobe steering values -0.22 and +0.22 correspond to the extreme directions within the range of directions with guaranteed performance. Assuming the radar is only operated in a way that lobe directions vary only within this range the system achieves

almost complete observability of the lobe direction and loss of lobe movement is detectable. Note though; that the method using logarithmic amplifiers has a slightly wider range of injective mappings from φ to the output.

If fast enough measurement equipment is used; the method using logarithmic amplifiers with full wave rectifiers, allows for perfect tracking of the lobe direction within a restricted range. The method not using logarithmic amplifiers does not have as wide an operating range, though the difference between the methods is very small.

4.3. Observer design

The output signal should ideally be measured only during pulses. Since pulses are short in time and average power measurements become uncertain for short averaging times, estimates of the lobe direction would be uncertain.
One way to improve estimates is to utilize a model of the observed system in a model based filter, such as the Kalman filter. However; for guaranteed optimality of Kalman filters the system variations and measurement noise must follow Gaussian distributions.
The lobe direction of the radar of interest does not follow a Gaussian distribution. Since there are no relevant dynamics in the AA and control signals can vary arbitrarily, the probability distribution of the lobe direction is constant. This can at best be considered a Gaussian distribution of infinite variance.
Thus; no model based filter can improve estimates of lobe direction based on the measurements used here.
Though a simpler special case of the Kalman filter can still be used to achieve optimal sensor fusion in the case that multiple measurement devices are installed, generating multiple observation variables.
Also; the more accurate estimate of the lobe direction is based on estimates of the phase difference between consecutive AEs and that kind of measurements can be improved through Kalman filtering.

In the following subsections a few different ways of applying Kalman filters to improve observer performance are demonstrated.
Section 4.3.1 explains in more detail why a Kalman filter will not improve direct estimates of the lobe direction as the variance is infinite.
Section 4.3.2 explains how Kalman filters can be used for sensor fusion, thus improving estimates of the lobe direction when using multiple sensors.
In section 4.3.3 a Kalman filter is applied as Phase locked loop filter, which could improve estimates of the phase of observed signals, which should indirectly improve the estimates of the lobe direction.

4.3.1. Kalman filtering of a single static observation variable

The system to be observed, the radar, can be modelled as a scalar state variable x - representing the lobe direction. Since the observing system will have no influence over -or even knowledge of- the control signals, these are characterized by the noise model and the deterministic control variables are set to constant 0.
Consider the system:

$$x[k+1] = Ax[k] + Bu[k] + Mv_1[k]$$
$$y[k] = Cx[k] + Du[k] + v_2[k]$$

Where:

$A = 1, \in R$
$B = 0, \in R$
$C = 1, \in R$
$D = 0$
$M = 1, \in R$
$k \in I \sim discrete\ time\ variable.$
$x[k] \in R,\ is\ a\ time\ dependent\ state\ variable.$
$u[k]\ \in R,\ control\ signal$
$v_1[k] \in R, is\ additive, white, zero\ mean\ Gaussian\ distributed\ disturbances.$
$v_2[k] \in R, is\ additive, white, zero\ mean\ Gaussian\ measurement\ noise.$

The Kalman filter for such a system is described by the following set of equations [16]:

$$\hat{x}[k|k] = \hat{x}[k|k-1] + K(y[k] - C\hat{x}[k|k-1] - Du[k])$$
$$K = (APC^T + MR_{12})(CPC^T + R_2)^{-1}$$
$$P = APA^T + MR_1M^T - (APC^T + MR_{12})(CPC^T + R_2)^{-1}(APC^T + MR_{12})^T\ >\ 0$$

Where the covariance matrices R_1, R_2 and R_{12} are:

$R_1 = \sigma_1^2, \in R$
$R_2 = \sigma_2^2, \in R$
$R_{12} = 0$

Calculating the Kalman filter with the given values gives:

$$P = P + \sigma_1^2 - (P)(P + \sigma_2^2)^{-1}(P)^T$$
$$\Rightarrow \sigma_1^2 - (P)(P + \sigma_2^2)^{-1}(P)^T = 0$$
$$\Rightarrow P^2 - \sigma_1^2(P + \sigma_2^2) = 0$$
$$\Rightarrow P = \frac{\sigma_1^2}{2} + \sqrt[2]{\sigma_1^2\sigma_2^2 + \frac{\sigma_1^4}{4}}, \in R^+$$

The typical movement of the lobe is very characteristic. The lobe direction varies in a way that to the observer will appear stochastic, with discrete jumps between arbitrary lobe directions with a constant probability distribution over feasible directions –as mentioned in 4.3.
Thus σ_1^2 will be much greater than σ_2^2:

$$\underset{\sigma_1^2 \gg \sigma_2^2}{\Longrightarrow} P = \frac{\sigma_1^2}{2} + \frac{\sigma_1^2}{2}\sqrt[2]{1 + \frac{4\sigma_2^2}{\sigma_1^2}} \approx \frac{\sigma_1^2}{2} + \frac{\sigma_1^2}{2}\left(1 + \frac{2\sigma_2^2}{\sigma_1^2}\right) = \sigma_1^2 + \sigma_2^2$$

Now consider the following:

$$\tilde{P} = cov(\tilde{x}[k|k]) = E\left[\tilde{x}[k|k]\tilde{x}^T[k|k]\right]$$

According to [15], this expression can be rewritten as:

$$\tilde{P} = \left(1 - \frac{\sigma_1^2+\sigma_2^2}{\sigma_1^2+2\sigma_2^2}\right)^2 (\sigma_1^2 + \sigma_2^2) + \left(\frac{\sigma_1^2+\sigma_2^2}{\sigma_1^2+2\sigma_2^2}\right)^2 \sigma_2^2$$

$$= \frac{\sigma_2^4(\sigma_1^2 + \sigma_2^2) + (\sigma_1^2 + \sigma_2^2)^2\sigma_2^2}{(\sigma_1^2 + 2\sigma_2^2)^2}$$

$$= \frac{(\sigma_1^2 + \sigma_2^2)[\sigma_2^4 + (\sigma_1^2 + \sigma_2^2)^2\sigma_2^2]}{(\sigma_1^2 + 2\sigma_2^2)^2}$$

$$= \frac{(\sigma_1^2 + \sigma_2^2)[\sigma_2^4 + (\sigma_1^2 + \sigma_2^2)^2\sigma_2^2]}{(\sigma_1^2 + 2\sigma_2^2)^2}$$

$$= \frac{\sigma_2^2(\sigma_1^2 + \sigma_2^2)[\sigma_2^2 + \sigma_1^2 + \sigma_2^2]}{(\sigma_1^2 + 2\sigma_2^2)^2}$$

$$= \frac{\sigma_2^2(\sigma_1^2 + \sigma_2^2)}{\sigma_1^2 + 2\sigma_2^2} = \sigma_2^2 \frac{1 + \sigma_2^2/\sigma_1^2}{1 + 2\sigma_2^2/\sigma_1^2} \approx \sigma_2^2, \qquad for\ \sigma_2^2 \ll \sigma_1^2$$

Now knowing the covariance of the state estimation error of both $\tilde{x}[k|k-1]$ and $\tilde{x}[k|k]$, i.e. P and $\tilde{P}$ respectively, comparing them generates some interesting results.

$$\frac{\tilde{P}}{P} = \frac{\left(\frac{\sigma_2^2(\sigma_1^2 + \sigma_2^2)}{\sigma_1^2 + 2\sigma_2^2}\right)}{\sigma_1^2 + \sigma_2^2} = \frac{\sigma_2^2}{\sigma_1^2 + 2\sigma_2^2} = \frac{\sigma_2^2/\sigma_1^2}{1 + 2\sigma_2^2/\sigma_1^2} < \frac{\sigma_2^2}{\sigma_1^2}$$

Considering the assumption that σ_1^2 is much larger than σ_2^2 the following conclusion can be drawn:

$$\frac{\tilde{P}}{P} = \frac{\sigma_2^2/\sigma_1^2}{1 + 2\sigma_2^2/\sigma_1^2} < \frac{\sigma_2^2}{\sigma_1^2} \ll 1$$

Simply put in words: The error variance of estimates $\hat{x}[k|k-1]$ is much larger than the error variance of estimates $\hat{x}[k|k]$.
The Kalman filter requires information from the current sample instant to achieve good estimates. Using information from previous state estimates gives practically no improvement on the quality of the state estimate.

4.3.2. Sensor fusion with multiple static variables using Kalman filtering

Using several sensors and implementing sensor fusion, the system can be modelled just as before –only with multiple sensors measuring the same state with independent zero mean Gaussian measurement noise.
Consider the system:

$$x[k+1] = Ax[k] + Bu[k] + M_1 v_1[k]$$
$$y[k] = Cx[k] + Du[k] + M_2 v_2[k]$$

Where:

$$A = 1 \qquad B = 0 \qquad C = \begin{bmatrix} 1 \\ \vdots \\ 1 \end{bmatrix}, \in R^{N\times 1}$$

$$D = 0 \qquad M_1 = 1, \in R \qquad M_2 = \begin{bmatrix} 1 & 0 & 0 \\ 0 & \ddots & 0 \\ 0 & 0 & 1 \end{bmatrix}, \in R^{N\times N}$$

$k \in R \sim discrete\ time\ variable.$
$x[k] \in R,\ a\ time\ dependent\ state\ variable, i.e.\ the\ lobe\ direction.$
$u[k] \in R,\ control\ signal$
$v_1[k] \in R, is\ additive, white, Gaussian\ distributed\ disturbances.$
$v_2[k] \in R^{N\times 1}, is\ additive, white, Gaussian\ measurement\ noise.$

The Kalman filter for such a system is described by the following set of equations [15]:

$$\hat{x}[k|k] = \hat{x}[k|k-1] + K(y[k] - C\hat{x}[k|k-1] - Du[k])$$
$$K = (APC^T + M_1 R_{12})(CPC^T + R_2)^{-1}$$
$$P = APA^T + M_1 R_1 {M_1}^T - (APC^T + M_1 R_{12})(CPC^T + R_2)^{-1}(APC^T + M_1 R_{12})^T$$

Where the covariance matrices R_1, R_2 and R_{12} are:

$$R_1 = \sigma_1^2, \in R$$

$$R_{12} = [0 \quad \cdots \quad 0], \in R^{1\times N}$$

$$R_2 = \begin{bmatrix} \sigma_{21}^2 & 0 & 0 \\ 0 & \ddots & 0 \\ 0 & 0 & \sigma_{2N}^2 \end{bmatrix}, \in R^{N\times N}$$

Appendix B shows that; for this system and the Kalman filter will have improved performance for an increasing number of sensors. Also, the Kalman filter will gain much performance on using the latest sample to form an estimate –rather than just using previous samples.

$$p = \frac{\sigma_1^2}{2}\left[1 + \sqrt[2]{1 + \frac{4}{\left(\frac{\sigma_1^2}{\sigma_{21}^2} + \frac{\sigma_1^2}{\sigma_{22}^2} + \cdots + \frac{\sigma_1^2}{\sigma_{2N}^2}\right)}}\right]$$

$$\tilde{p} = \frac{p}{1 + \Omega p} < p$$

$$\Rightarrow \frac{\tilde{p}}{p} = \frac{\lambda_2^2}{\sigma_1^2 n}$$

The analysis of sensor fusion through Kalman filtering found in appendix B shows that this method can efficiently decrease the variance of estimates using any combination of sensors. There can be any number of sensors. The sensors can have any combination of stochastic noise characteristics. Practically identical sensors can be used or a combination of various kinds of sensors can be used. Sensors can even measure different physical quantities as long as the fused estimates are estimates of the same quantity.

The analysis also shows that, for the particular application in mind, there is a great advantage in implementing the Kalman filter such that all samples up to the current measurement are used rather than just previous samples.

This is an efficient way of decreasing estimate variance when there are many sensors available. Though using multiple sensors increases the complexity of the system and is a practical inconvenience when it comes to installing all sensors and data acquisition hardware needed to gather and process all measurements.
Unless there exist circumstances making several sensors necessary for other reasons, it would be preferable to use a measurement and filtering technique which gives low enough estimate variance with a single or a few sensors.
Section 4.3.3 describes a measurement setup which achieves complete observability and is capable of low variance estimation with two microwave receivers connected to a phase detector circuit.

4.3.3. Kalman filter-based phase-locked loop filter for pulse measurements

Assuming that each pulse is sampled by two independent receivers, to be compared in phase, it is very important to measure the phase at both receivers accurately. A Kalman filter with an accurate model of the signals phase and its time derivatives can form a PLL filter. Such a filter could improve the phase estimation accuracy at each sample, significantly improving lobe direction estimates.
As mentioned in section 2 this method has been subject to some research already. In carrier signal phase tracking a PVA model, which is basically a double integrator, is commonly used to describe the dynamics of the carrier signal [12],[13],[14],[16],[17] and [18].

This technique can be very effective in reducing phase noise in phase tracking applications, thus it has some potential for use in this problem. Consider the following measurement scenario:

since not only the frequency of the signal is to be estimated from samples but also the phase of the signal; each pulse sent out from the radar would be sampled at a sampling frequency much higher than the signal frequency.
The samples are passed through a PLL based on Kalman filtering to reduce phase noise. Finally the PLL-filtered signal can be passed on as a low noise estimate of the radar output from the sensor that recorded it, the low noise estimates from two sensors can then be passed through a phase detection circuit to give an estimate of the phase difference between the two sensor readings.

Figure 10 describes the mapping of phase difference between two sensor signals to the output level of a phase detector comparing the two signals. These two sensors need to be positioned close to the AA, in front of the two AEs furthest out on the sides of the AA.
If these two signals are sampled by two synchronized sampling devices and then passed through PLL Kalman filters: They can be passed as the two outputs to a phase detector.
The phase detector would then give an output depending on the phase difference between the two measured signals, thus also the lobe direction, according to the mapping in figure 10. This output could then me measured as a voltage level allowing simple software to calculate an estimated lobe direction.

The PVA model used in the Kalman filter is based on the modelling in [17] with the slight modification that the amplitude of the signal is not included in the model:

$$x(k+1) = \begin{bmatrix} x_1(k+1) \\ x_2(k+1) \\ x_3(k+1) \end{bmatrix} = \underbrace{\begin{bmatrix} 1 & T & \frac{T^2}{2} \\ 0 & 1 & T \\ 0 & 0 & 1 \end{bmatrix}}_{A} x(k) + \underbrace{\begin{bmatrix} 0 \\ 0 \\ 1 \end{bmatrix}}_{B} sin(\omega k T) + \underbrace{\begin{bmatrix} 0 \\ 0 \\ 1 \end{bmatrix}}_{M} v_1(k)$$

$$y(k) = \underbrace{[1 \quad 0 \quad 0]}_{C} x(k) + v_2(k)$$

Where:

The column vector which is multiplied with a sine-term is an uncontrolled signal driving the process.

$x(k) \in R^3$
$x_1(k), x_2(k), x_3(k)$ *correspond to the phase, frequency and frequency time derivative respectively.*

$y(k) \in R$ *is the meassurement signal.*

$v_1(k) \in R$ *and* $v_2(k) \in R$ *are process disturbances and measurement noise respectively, they can both be considered zero mean, Gaussian distributed stochastic.*

ω *is the frequency of the observed radar pulse.*

B is the matrix through which the driving sine signal, with unknown phase, is introduced to the system.

M is the matrix through which the process disturbances are introduced.

T *is the sampling time.*

Once again the Kalman filter is calculated based on the equations [15]:

$$\hat{x}[k|k] = \hat{x}[k|k-1] + K(y[k] - C\hat{x}[k|k-1] - Du[k])$$
$$K = (APC^T + MR_{12})(CPC^T + R_2)^{-1}$$
$$P = APA^T + MR_1M^T - (APC^T + MR_{12})(CPC^T + R_2)^{-1}(APC^T + MR_{12})^T$$

Where the covariance matrices R_1, R_{12} and R_2 are:

$$R_1 = \sigma_1^2, \quad R_{12} = 0, \quad R_2 = \sigma_2^2$$

Which would yield the DARE:

$$P = \begin{bmatrix} 1 & T & \frac{T^2}{2} \\ 0 & 1 & T \\ 0 & 0 & 1 \end{bmatrix} P \begin{bmatrix} 1 & 0 & 0 \\ T & 1 & 0 \\ \frac{T^2}{2} & T & 1 \end{bmatrix} + \begin{bmatrix} 0 & 0 & 0 \\ 0 & 0 & 0 \\ 0 & 0 & 1 \end{bmatrix} - \left(\begin{bmatrix} 1 & T & \frac{T^2}{2} \\ 0 & 1 & T \\ 0 & 0 & 1 \end{bmatrix} \begin{bmatrix} P_{11} \\ P_{21} \\ P_{31} \end{bmatrix} \right) (P_{11} + \sigma_2^2)^{-1} \left(\begin{bmatrix} 1 & T & \frac{T^2}{2} \\ 0 & 1 & T \\ 0 & 0 & 1 \end{bmatrix} \begin{bmatrix} P_{11} \\ P_{21} \\ P_{31} \end{bmatrix} \right)^T$$

As mentioned this method would require much faster sampling than just one sample per pulse. The pulses would need to be sampled at high GHz frequencies causing implementation issues both in numerical calculations of the DARE and in the choice of hardware for sampling and processing the signals. Though if using an FPGA device, the desired signal processing speed should be possible to achieve.

Obviously this approach is only viable if very high performance is necessary, since there are other methods which are much simpler and much less demanding in terms of hardware capabilities. Though it is by far the most relevant use of Kalman filtering to estimate the lobe direction based on the available signals. For high angular resolution tracking of the lobe direction this approach might even be necessary to get the desired signal quality.

4.4. Error analysis of model

There are a few known sources of modelling errors:

1. Reflections from nearby metal objects (especially the sensor fixture) may cause disturbances.
2. The radar has the ability of phase control in the vertical dimension of the antenna, for height estimates of targets. This can cause significant disturbances unless compensated for.
3. Pulse compression is a method to increase the resolution of the radar through signal processing. A description of this method is out of the scope of this thesis.
   The pulse compression affects the signal perceived by the sensors in the supervision system yet it is not modelled in the simulation used to evaluate the design of the supervision system.

Reflections can be very hard to model and since there are no dynamics in the developed model there is no way to filter out such disturbances unless the control sequence to the system is known. Though for the chosen implementation this is not a problem. Reflections would be constant, thus causing biased estimates of the lobe direction. Though the implemented system observes changes in the estimated lobe direction and these will be unaffected by estimate bias.

Vertical beam steering can be compensated for by generalizing the current solution to include vertically aligned sensor pairs as well as horizontal pairs. Vertical beam steering is achieved through dividing the antenna into an upper half and a lower half and controlling the phase shift between lower half AEs and upper half AEs. Placing one sensor at the top of the antenna and one at the bottom, while also making some modifications to the model, will allow estimation of lobe elevation if necessary.
The same approach used to estimate the azimuth of the lobe can be used to estimate the elevation of the lobe.
Arranging the sensor pairs for elevation and azimuth estimation orthogonally in the plane of the antenna surface will also make their respective outputs linearly independent.
This kind of sensor configuration is not implemented at Saab as this disturbance is expected to be small and the mechanical mounting of sensors would become more problematic.

Pulse compression changes the output, from a sine wave with constant frequency to a sine wave with a frequency decreasing over time. However, this is important mainly when using the Kalman filter described in section 4.3.3. and that Kalman filter includes pulse compression in the model.
In the simpler system implemented at Saab, pulse compression should not produce significant disagreement with the model.

5. Implementation of the supervision system

The goal of this thesis project was to implement a supervision system capable of detecting loss of lobe movement. Based on the investigated theory for estimating lobe direction it was assumed that a simple configuration of receiving antennas connected to a radio frequency average power sensor should be sufficient equipment for the implementation.
By sampling the RF average power repeatedly and calculating the variance of the last few samples, loss of lobe movement was expected to manifest through a very low variance estimate.

A system description was written at Saab for internal reference to the system design and its function. The system description can be found in Appendix B of this report.

Briefly summarized the implementation of the system consisted of: Ordering RF cables, combiner circuits, RF average power sensors and attenuators; specifying and ordering custom sensor mountings; installing the new equipment; specifying and aiding in the development of software for automatic monitoring of the lobe movement.

A complete system was installed according to the measurement method and monitoring algorithm described and suggested in this work.

It is obvious in figure 13 that sensor pairs are not actually placed at the ends of the antenna array. This picture shows the system as it was configured during initial testing. During these tests the idea was to keep sensors just as far apart as the antenna elements on the antenna array.
Although the sensor distribution shown in figure 13 doesn't provide the desired output characteristics for tracking of the lobe direction it was definitely adequate for detecting loss of lobe movement.

Since the equipment used in this work is not fast enough to perform lobe direction tracking, that concept was not tested. Only a simple detection of loss of lobe movement was verified.

Figure 13: Close up of sensor mountings.
1 – Receiving antenna pair in plastic encasing.
2 – Attenuators protecting the power combiner.
3 – Power combiner.
4 – Second sensor mounting.

5.1. Fault state description of the radar

The method of detecting a stationary lobe through the variance of RF average power estimates is not perfect. A few complementary rules are required to correctly model the states of the antenna such that normal operation can be efficiently distinguished from faulty operation. Consider the following assumption:

The variance of the RF average power can either be high or low.

- Low variance can be caused by:
  - Stationary lobe
  - No transmission / passive mode
  - Faulty / disconnected sensor

- High variance can be caused by:
  - Smooth scanning
  - Piecewise smooth scan
  - Instantaneous jumps between two or more tracks

This is a list of the different states of the antenna and their association with loss of lobe movement. In order to efficiently detect loss of lobe movement without risking false alarms the number of measured variables must be increased to make the modelled system observable –ie; other than estimating the variance of the signal from the supervision system it is also necessary to know if the transmission is turned on.

In order to distinguish a stationary lobe from the different states causing low variances it is sufficient to measure the signal level on the lowest possible resolution -high or low. As long as low variance levels are only allowed when running the antenna in passive mode, there is no risk of losing lobe movement without detecting it.
By use of multiple sensor pairs and comparison of signal levels it is also possible to distinguish passive mode from single sensor faults.

Although this model is sufficient to detect loss of lobe movement, there are still other possible scenarios which can produce radiation distribution similar to that of a stationary lobe, while passing for moving lobe transmission.
Consider for example the case that the lobe alternates between two directions. If these directions are far enough apart the variance of the estimated lobe direction will be high, though this kind of transmission could potentially cause unacceptably high electric field strengths in certain nearby areas.
This is one of a few examples of very unlikely scenarios which require a much more detailed definition of transmission scenarios which can cause unacceptable electric field strengths. Such a definition of faulty transmission would also require a very precise estimation of the lobe direction to make possible the detection of such transmission.

5.1.1. Improved fault state description

The safest scenario would of course be the more conservative approach to not allow transmission at all in any direction with a limit on exposure time. Though, this would only allow transmission in a few directions with 10° tilt of the radar antenna while transmission with 5° tilt would be impossible.
This section describes a possible improvement on the algorithm for detecting loss of lobe movement. The described method was not implemented because it requires high precision tracking of the lobe direction while the implemented algorithm showed sufficient performance without tracking of lobe direction.

For perfect transmission supervision each transmission direction needs to be observed independently of others. Since the terrain at the test range is uneven, the sensitivity to transmission in different directions varies.
The maximum exposure times allowed for different average electric field strengths are known and can be found in [3] and average electric field strengths in the terrain are known for all possible transmission directions and can be found in [2].
If each transmission direction is assigned an output, independent of all other outputs, these can be amplified and integrated such that each output will cross a threshold as the corresponding transmission direction has been overexposed.

$$y_n^{res}[k] = y_n^{res}[k-1] + C_n \cdot y_n[k]$$

Where:

$C_n = \frac{pulse\ frequency}{max\ exposure\ time\ in\ direction\ n} \in R \sim$ *Weighting factor scaling the residual to become 1 as the corresponding transmission limit is reached.*

$y_n \in \{-1.1\} \sim$ *Negative output for no transmission in direction n, positive otherwise.*

5.2. System identification

Before the antenna went through final calibrations it was tested with reduced transmission power. This allowed safe transmission without the supervision system installed at the test rig. During these tests, measurements were performed to evaluate the proposed solution and to collect data for a rough estimate of threshold parameters.

The system identification experiment was not an actual system identification, system parameters were not appropriately quantified. During the experiment sensors where moved between different positions in an attempt to determine whether the measured output was qualitatively similar to the output predicted by the model.
That is; the measured output was plotted during transmission with a smooth scanning pattern and the plots were then compared to a cosine signal.
Since the identification experiment was simplified to a rough qualitative evaluation of the system, some important tuning parameters were not determined before this experiment;

- The sample interval of the average power sensor was not synchronized to the pulse interval of the radar. Sampling was performed only as fast as was possible with polling from a windows based control application. (Much slower than radar pulse intervals and with a large amount of jitter)
- Sensor positions were measured only at approximately one centimeter of precision.

- Actual power levels where not measured. Only dBm (where the measured power is expressed as a gain relative to 1 mW) outputs of the power sensor were registered and these were not transformed to actual power levels or electric field strengths.

As a consequence of the many remaining uncertainties the method was only evaluated to the degree that it was deemed sufficient for satisfying the requirements. As the antenna is finished; the first transmissions will have to be limited in such a way that the supervision system is not required, since these first transmissions will have to be used to calibrate and verify the supervision system.

The output was expected to show distinct amplitude dependence on the phase control. To test the hypothesis of an amplitude modulated output the radar was configured to scan as large an area as was possible under current safety restrictions. The output and the phase control was then recorded and the data was time stamped.

After confirming that the output followed expectations for normal operation the lobe was locked for a brief time in the direction of the antenna normal. The measured output and the phase control were once again recorded and compared.
As can be seen in figure 14, the measured output varies distinctly with the lobe movement and there was a clear indication that loss of lobe movement would be easily detectable.

Note that the output seems to vary as the cosine of twice the control phase, which is to be expected because, during this test, sensors were placed twice as far apart as is suggested for the final product. The reason that the valleys of the output look so unpleasing is that the output was over attenuated, in order to protect the average power sensor, such that noise became dominant for these lower outputs.
For the final tests the sensors will be mounted closer together and less attenuation will be used.

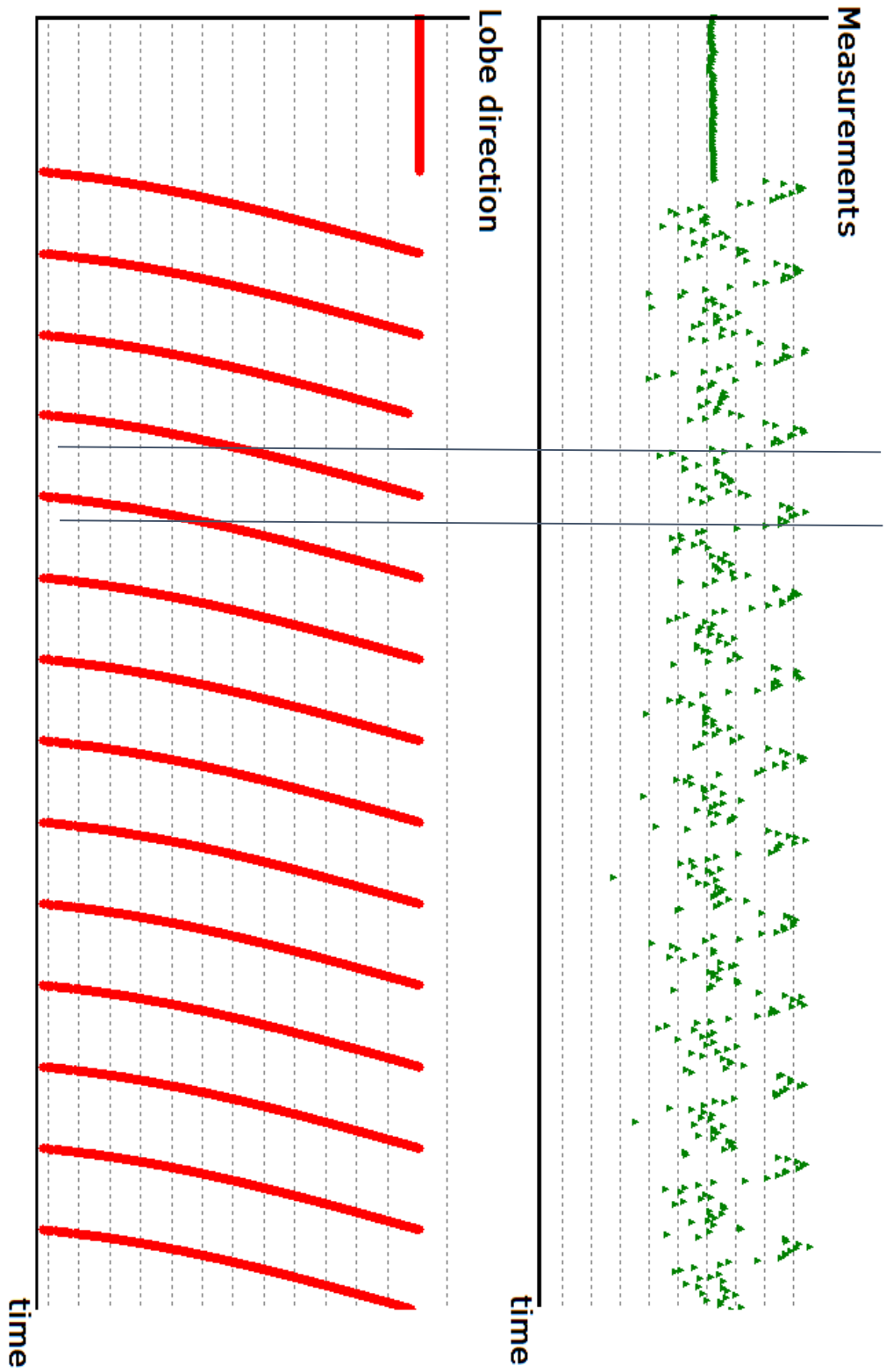

Figure 14: Top of figure, green plots – measured output over time.
Bottom of figure, red plots – lobe direction reference value, read from antenna control bus.
First; the lobe direction was locked along the antenna bore sight for a short time (constant measurements and reference value), and finally the same area was scanned again 14 times.
The area scanned was a large portion of the sector to the left of antenna bore sight.

5.3. Configuration and verification

This section gives an overview of the verification of the supervision system. The function of the system is briefly described and a procedure for verifying the functionality is provided. A detailed documentation of the verification can be found in [20].

During calibration and verification, transmission must be time limited to assure safe transmission. Before the supervision system can be considered fully operational its function must be verified according to the following list:

1. Alarm is triggered within the specified time, when the lobe is stationary.
2. The alarm generates a signal which successfully shuts down the radar.
3. (The alarm follows specifications equally well for all loss of lobe movement in any direction)
4. The alarm is triggered by unacceptably narrow scanning areas.
5. The alarm is not triggered in passive mode.
6. There are no other false alarms.

7. (Disconnected sensors are detected as faulty sensors)
8. (Detection of faulty sensors generates a warning signal)

Requirements 7 and 8 are not actually requirements, though they are desired functions. Initially the software implementation of the supervision system must utilize the threshold deduced from the data of the early experiments. Verification should be performed with this threshold, meanwhile data should be recorded during all parts of the verification. The data recorded during verification can then, if necessary, be used to fine tune the threshold offline. In case an adjustment of the threshold or sensor position is made, points 1,3,4,5 and 6 must be verified again.
Before verification, the parameters of the supervision system must be estimated.

During all parts of calibration and verification where the radar is on; one operator must constantly monitor real time plots of measurements and if necessary turn off the radar power in case of unexpected outputs or failure of the supervision system.

Calibration
• Make sure sensors are connected and software running. • Configure radar for passive mode. • Start radar and operate under passive mode for 1 min. • Configure the radar to scan smoothly over a large sector. • Transmit with smooth scanning for 30 seconds. • Extract recorded data to determine a power level threshold for setting the passive mode state as active in the supervision system and verify that active transmission generates significantly higher power levels than passive mode operation. • Reconfigure expected power levels in sensor settings.

Test scenario 1: Verification of point 1 and 2
• Configure the radar to scan smoothly over a large sector. • Start transmission. • Repeat the operation established in the early experiments for locking the lobe direction. • Check that the transmission power is cut by the supervision system within 10 s of stationary lobe direction.

Test scenario 2: Verification of point 4
• Configure the radar to scan smoothly over a large sector. • Start transmission. • Scan sector for 2 minutes. • Configure the antenna to scan a sector with minimum size according to radar specifications. • Check that the transmission power is cut by the supervision system within 10 s of stationary lobe direction.

Test scenario 3: Verification of point 5 and 6

- Configure the radar to scan smoothly over a full sector.
- Start transmission.
- Run transmission for 5 min.
- Configure the radar to scan as small a sector as possible, in antenna normal direction.
- Scan minimum sector for 2 min.
- Configure the radar to scan as small a sector as possible, in wide angle lobe direction.
- Scan minimum sector for 2 min.
- Configure radar for passive mode.
- Operate radar under passive mode for 2 min.
- Repeat the operation established in the early experiments for locking the lobe direction.
- Check that the transmission power is cut by the supervision system within 10 s of stationary lobe direction.

Test scenario 4: Verification of point 3

- Configure the radar to scan smoothly over a full sector.
- Start transmission.
- Fix lobe in direction $-\pi/3$ radians from the antenna normal.
- Check that the transmission power is cut by the supervision system within 10 s of stationary lobe direction.

- Repeat for $-\pi/6$, $\pi/6$ and $\pi/3$ radians from bore sight.

Test scenario 5: Verification of point 7 and 8

- Disconnect one receiving antenna element.
- Configure the radar to scan smoothly over a full sector.
- Start transmission.
- Check that fault sensor warning is triggered.

- Disconnect one RF average power sensor.
- Configure the radar to scan smoothly over a full sector.
- Start transmission.
- Check that fault sensor warning is triggered.

6. Discussion

The main problem of developing the supervision system can be divided into two sub problems; that of measuring the electric field in a practical way such that good observability is achieved and that of filtering the observations such that estimates of the lobe direction can be made with satisfying accuracy.

The problem of measuring the electric field was solved in a way that was conceptually unexpected. Initial studies of near-field characteristics and diffraction of AAs unveiled very complex electric fields, suggesting very low observability, requiring a large sensor array to observe the states of a large AA.
However, it seems that by measuring very close to the AA and measuring phase rather than magnitude; the problem was more manageable.

The problem of filtering measurements to achieve good estimates of the lobe direction also seemed to be a hard problem at first. Initially, the approach was to first get an estimate of the lobe direction then to use a Kalman filter to suppress noise.
It was quickly realized that, in most commonly used search modes, the AA behaved in a way that made previous lobe directions have no significant effect on the current lobe direction, thus making Kalman filtering of lobe direction estimates useless.
The best use of a Kalman filter for this problem seem to be to use it for improving estimates of the phase difference between AEs. Though this approach requires high speed sampling of radar pulses and can only be motivated for high performance solutions where tracking of lobe direction is required at the same resolution as that of the antenna control.

The solution which is theoretically investigated in this work requires sampling at high GHz frequencies and non-trivial signal processing at corresponding speeds. This brings a risk of expensive and complicated implementation. However the specific problem at hand can be satisfactorily solved through a simplified approach.

For detection of stationary lobe it is not necessary to have accurate estimates of lobe direction as long as differences in direction can be detected between samples.
The output model suggests that the output will be a sine signal with amplitude dependent on the phase shift between consecutive AEs and by extension the lobe direction. Thus by measuring the average power over pulses of the output one can get a rough estimate of the lobe direction. Calculating the variance of recent samples it is then possible to detect a stationary lobe as a low variance estimate.
This simplified approach can be easily and cost efficiently implemented using a RF average power sensor. It is sufficient for detecting a stationary lobe, though not for accurate tracking of lobe direction.
Implementation of the more complex system, seemingly capable of tracking the lobe direction, is out of the scope of this work.

The simplified approach is fully capable of detecting a stationary lobe, though some other possible fault modes are described in this thesis that are not detectable through the variance of the output. It is theoretically possible that the lobe could jump back and forth between only two directions far apart, this would cause high output variance with potential for unsafe electric field strengths in the test range.
This problem could be solved by the higher performance approach if deemed necessary. However; the investigations that motivated this work have thoroughly considered the possible

fault modes in their probability of occurrence and their severity and the conclusion is that safe transmission can be guaranteed with automatic detection of a stationary lobe only.

7. Conclusions

Since the simple method based on average power measurements satisfies requirements it was chosen and implemented. Suitable components were purchased and mounted at the system rig where the supervision system was tested with the real ERIEYE antenna.
Initial tests gave promising results and software was developed and installed for full functionality of the supervision system.

For further work it could be interesting to investigate the possibility of implementing a phase detector based on logarithmic amplifiers, full wave rectifiers, a mixer and kalman filtering. This would require choosing a suitable platform, optimizing the algorithm for implementation on the platform and developing a method for evaluating the performance of the implementation.
The choice of platform for such a system was not in the scope of this thesis. Though there is a device from National Instruments called USRP that is a promising candidate for this platform. Further assessment of this platform is required to determine whether this platform is capable of Kalman filtering the output signal at the required speed.
Even without Kalman filtering of the signal the use of a USRP could be a significant improvement since it would allow allocating most, if not all of the system software in the FPGA of the USRP. This would increase detection speed and shorten the latency from detection of a stationary lobe in the measurement equipment to actual disconnection of transmission power.

As previously mentioned this solution is geared towards a strange problem, probably never encountered in readily developed radar systems and rarely in the actual development of radar systems. However, it should be useful in other test rigs where the lobe direction has to be confirmed in real time by observations of actual output rather than control signals.
It could also be interesting to compare the theoretical performance of the suggested method of Kalman filtering samples of the radar pulse from two sensors and then comparing the phase of the filtered signals, against more conventional DOA techniques using larger arrays of sensors.

References

A few of the references are internal documents at Saab. These documents are not publically available, however they are still included because of their relevance to Saab employees reading the report. All of the Saab documents in the reference list are marked with an asterisk.

1. ARBETARSKYDDSTYRELSENS FÖRFATTNINGSSAMLING
   AFS 1987:02 – "*Högfrekventa elektromagnetiska fält*", (1987, August 20)

2. ***** 16/0363-E/FCP104422; "Erieye: *Elektrisk fältstyrka i terrängen kring systemmätsträckan i Kallebäck*"

3. ***** 29/0363-FCX90112/13; "*Mätning av radiofrekvent strålning från systemrigg Erieye Regina, fullbestyckad DOU*"

4. Ashkan Panahi, "*Consistency analysis and regularization parameter selection for direction-of-arrival estimation*", department of Signals and Systems, Chalmers University of technology, Gothenburg, Sweden, 2010.

5. Fredrik Athley, "*Angle and Frequency Estimation Using Sensor Arrays*", department of Signals and Systems, Chalmers University of Technology, Gothenburg, Sweden, 2001.

6. Raviraje Adve. (2013, July 28). *Direction of Arrival Estimation* [Online]. Available: http://www.comm.utoronto.ca/~rsadve/Notes/DOA.pdf

7. Benjamin M.W. Baggett, "*Optimization of Aperiodically Spaced Phased Arrays for Wideband Applications*", Faculty of the Virginia Polytechnic Institute and State University, Blacksburg Virginia, USA, 2011.

8. Lianlin Li, wenji zhang and Fang Li , "*The Design of Sparse AA*", Institute of Electronics, Chinese Academics of Sciences, Beijing, China, 2008.

9. Jenny Hilbertsson, Josefina Magnusson, "*Simulation and Evaluation of an Active Electronically Scanned Array (AESA) in Simulink*", department of Signals and Systems, Chalmers University of Technology, Gothenburg, Sweden, 2009.

10. Doren W. Hess, "*A SIMPLE ANALYSIS OF NEAR-FIELD BORESIGHT ERROR REQUIREMENTS*", MI Technologies, Duluth GA, USA, 2012.

11. Glen D. Gillen and Shekhar Guha, "*Modeling and propagation of near-field diffraction patterns: A more complete approach*", USAF Research Labs.,Ohio, USA, 2004, vol.72.

12. Mario Gomez Arias, "*Adaptive Kalman Filter-Based Phase-Tracking in GNSS*", Institute for Communications and Navigation, Technische Universität München, München, Germany, 2010.

13. Patapoutian, Ara, "On phase-locked loops and Kalman filters", *Communications, IEEE Transactions on* , vol.47, no.5, pp.670,672, May 1999

14. Cillian O'Driscoll and G´erard Lachapelle, "*Comparison of Traditional and Kalman Filter Based Tracking Architectures*", department of Geomatics Engineering, Schulich School of Engineering, University of Calgary, Calgary, Alberta, Canada, 2009.

15. Torkel Glad and Lennart Ljung, "Kalman Filters", *CONTROL THEORY Multivariable and Nonlinear Methods*, 1st ed. London, UK: Taylor & Francis, 2000, ch. 5, sec. 7, pp.137-138.

16. De Brabandere, K.; Loix, T.; Engelen, K.; Bolsens, B.; Van Den Keybus, J.; Driesen, J.; Belmans, R., "Design and Operation of a Phase-Locked Loop with Kalman Estimator-Based Filter for Single-Phase Applications," *IEEE Industrial Electronics, IECON 2006 - 32nd Annual Conference on* , vol., no., pp.525,530, 6-10 Nov. 2006

17. Gal, J.; Campeanu, A.; Nafornita, I., "Estimation of Chirp Signals in Gaussian Noise by Kalman Filtering," *Signals, Circuits and Systems, 2007. ISSCS 2007. International Symposium on*, vol.1, no., pp.1,4, 13-14 July 2007

18. Robert Grover Brown, Patrick Y. C. Hwang, in *Introduction to Random Signals and Applied Kalman Filtering*, 4:th ed. New Jersey: John Wiley & Sons, Inc., 2012, ch. 4, pp. 167.

19. J. Cowles, b. Gilbert (2001, October 5). *Accurate Gain/Phase Measurement at Radio Frequencies up to 2.5 GHz* [Online]. Available: http://www.http://www.analog.com/library/analogdialogue/archives/35-05/ad8302/

20. ***** 1/10265-LPA201191/6; *"ERIEYE rig, Verification of safety functions"*

21. T.S. Söderström and Petre G. Stoica, "Kalman Filters", *System Identification*, 1st ed. University of Michigan, USA: Prentice Hall, 1989, App. 3.

Appendix A, Matlab script for simulating the output

```
%% This script was used to run varying simulations scenarios as part of a
% master thesis. The simulations concern a phase detector system used for
% monitoring the lobe movement of an AESA radar.
%
% Since the radar antenna is intended for military applications parameters
% such as operating frequency and transmission power can not be revealed.
% Therefor physical quantities related to such information are not
expressed
% in S.I. units. All distances, such as d0 and d1, are expressed in terms
% of wavelengths of the transmitted radar pulses.
%
% Author: Kim Viggedal
% Last updated: 2013-09-30
%

%% Antenna parameters
%
N=              % Number of antenna elements
d0=             % wavelengths between consecutive antenna elements
d1=             % wavelengths from antenna array to receiver

%% Initialize simulation
%
K=1800;                           % number of lobe directions to simulate for
ctrlPhase=-pi/3:2*pi/3/K:pi/3;  % range of control signal values
recSig1=zeros(1,K);               % allocate memory for output 1
recSig2=zeros(1,K);               % allocate memory for output 2

%% Run simulation
%
for index=0:1:X             % Replace X with no. of AEs (antenna elements)
elOffSet=index;             % Sensor position offset from antenna middle
elNums=1:N/2+elOffSet;
%% Antenna model
% Calculates the phase and amplitude from each antenna element as observed
% from two different positions at each side of the antenna.

%
array=[elNums(end:-1:1)-ones(1,N/2+elOffSet) elNums(1:end-2*elOffSet)];

% Phase delay from distance
delays1=2*pi*sqrt(((d0*array).^2)/4+(d1*ones(1,N)).^2);
delays2=2*pi*sqrt(((d0*array(end:-1:1)).^2)/4+(d1*ones(1,N)).^2);
% Amplitude attenuation
amps1=ones(1,N)./(4*pi*((d0*array).^2+(d1*ones(1,N)).^2));
amps2=ones(1,N)./(4*pi*((d0*array(end:-1:1)).^2+(d1*ones(1,N)).^2));



%% Measured output
% Calculates the output for two cases of signal processing:
%   1) The two observed signals are simply subtracted and the absolute
%   value of the difference is considered the output.
%   2) The absolute value of each observation is logarithmically amplified.
%   Then the difference of the two resulting signals are considered the
%   output.
%
% The two outputs are then normalized.

    % Scale amplitude
    amps1=amps1/max(amps1);
```

```
    amps2=amps2/max(amps2);
    for k=1:K
        recSig1(k)=(amps1.*exp(j*(delays1+(1:N)*ctrlPhase(k))))*ones(N,1);
        recSig2(k)=(amps2.*exp(j*(delays2+(1:N)*ctrlPhase(k))))*ones(N,1);
    end
    % Final output
    output(index+1,:)=abs(recSig1)-abs(recSig2);
    logOutput(index+1,:)=(log(abs(recSig1))-log(abs(recSig2)));
    % Final output scaled
    output(index+1,:)=output(index+1,:)/max(output(index+1,:));
    logOutput(index+1,:)=logOutput(index+1,:)/max(logOutput(index+1,:));
end

%% Plot
%
figure
subplot(2,2,1)
plot(delays1)
axis tight
subplot(2,2,2)
plot(amps1)
axis tight
subplot(2,2,3)
plot(delays2)
axis tight
subplot(2,2,4)
plot(amps2)
axis tight

figure
subplot(1,2,1)
surf(output)
shading interp
axis tight
subplot(1,2,2)
surf(logOutput)
shading interp
axis tight

figure
plot(-1/3:2/3/K:1/3,[output(X+1,:) 0])    % Replace X with number of AEs
axis tight

figure
plot(-1/3:2/3/K:1/3,[logOutput(X+1,:) 0]) % Replace X with number of AEs
axis tight

clear
```

Appendix B, Sensor fusion analysis

Using several sensors and implementing sensor fusion, the system can be modelled just as before –only with multiple sensors measuring the same state with independent zero mean Gaussian measurement noise.
Consider the system:

$$x[k+1] = Ax[k] + Bu[k] + M_1 v_1[k]$$
$$y[k] = Cx[k] + Du[k] + M_2 v_2[k]$$

Where:

$$A = 1, \in R \qquad B = 0 \qquad C = \begin{bmatrix} 1 \\ \vdots \\ 1 \end{bmatrix}, \in R^{N \times 1}$$

$$D = 0 \qquad M_1 = 1, \in R \qquad M_2 = \begin{bmatrix} 1 & 0 & 0 \\ 0 & \ddots & 0 \\ 0 & 0 & 1 \end{bmatrix}, \in R^{N \times N}$$

$k \in R \sim discrete\ time\ variable.$
$x[k] \in R,\ a\ time\ dependent\ state\ variable, i.e. the\ lobe\ direction.$
$u[k] \in R,\ control\ signal$
$v_1[k] \in R, is\ additive, white, Gaussian\ distributed\ disturbances.$
$v_2[k] \in R^{N \times 1}, is\ additive, white, Gaussian\ measurement\ noise.$

The Kalman filter for such a system is described by the following set of equations [16]:

$$\hat{x}[k|k] = \hat{x}[k|k-1] + K(y[k] - C\hat{x}[k|k-1] - Du[k])$$
$$K = (APC^T + MR_{12})(CPC^T + R_2)^{-1}$$
$$P = APA^T + M_1 R_1 {M_1}^T - (APC^T + M_1 R_{12})(CPC^T + R_2)^{-1}(APC^T + M_1 R_{12})^T$$

Where the covariance matrices R_1, R_2 and R_{12} are:

$$R_1 = \sigma_1^2, \in R$$

$$R_{12} = [0 \quad \cdots \quad 0], \in R^{1 \times N}$$

$$R_2 = \begin{bmatrix} \sigma_{21}^2 & 0 & 0 \\ 0 & \ddots & 0 \\ 0 & 0 & \sigma_{2N}^2 \end{bmatrix}, \in R^{N \times N}$$

$$P = P + R_1 - PC^T(CPC^T + R_2)^{-1}CP^T$$

$$\Rightarrow p^2[1 \quad \cdots \quad 1]\left[\begin{bmatrix}1\\ \vdots \\ 1\end{bmatrix}[1 \quad \cdots \quad 1]p + R_2\right]^{-1}\begin{bmatrix}1\\ \vdots \\ 1\end{bmatrix} = \sigma_1^2$$

Now consider the following substitutions: $\gamma_i = \frac{\sigma_{2i}^2}{p},\ \Gamma = \begin{bmatrix}\gamma_1 & 0 & \cdots & 0\\ 0 & \ddots & & \vdots \\ & & \gamma_i & \\ \vdots & & \ddots & 0\\ 0 & \cdots & 0 & \gamma_N\end{bmatrix} = \frac{1}{p}R_2$

$$\Rightarrow \Gamma^{-1} = pR_2^{-1}$$

$$\Rightarrow p^2[1 \quad \cdots \quad 1]\left[\left(\begin{bmatrix}1\\ \vdots \\ 1\end{bmatrix}[1 \quad \cdots \quad 1] + \Gamma\right)p\right]^{-1}\begin{bmatrix}1\\ \vdots \\ 1\end{bmatrix} = \sigma_1^2$$

$$\Rightarrow p[1 \quad \cdots \quad 1]\left[\begin{bmatrix}1\\ \vdots \\ 1\end{bmatrix}[1 \quad \cdots \quad 1] + \Gamma\right]^{-1}\begin{bmatrix}1\\ \vdots \\ 1\end{bmatrix} = \sigma_1^2$$

Note that the matrix inverse above can be rewritten according to the inversion lemma [21]:

$$[CC^T + \Gamma]^{-1} = \Gamma^{-1} - \Gamma^{-1}C[1 + C^T\Gamma^{-1}C]^{-1}C^T\Gamma^{-1}$$

Now consider the following substitutions: $C^T\Gamma^{-1}C = \left(\sum_{i=1}^{N}\frac{1}{\sigma_{2i}}\right)p = \Omega p$

$$\Rightarrow \Gamma^{-1} - \Gamma^{-1}C[1 + C^T\Gamma^{-1}C]^{-1}C^T\Gamma^{-1} = \Gamma^{-1} - \Gamma^{-1}C[1 + \Omega p]^{-1}C^T\Gamma^{-1}$$
$$\Rightarrow pC^T[\Gamma^{-1} - \Gamma^{-1}C[1 + \Omega p]^{-1}C^T\Gamma^{-1}]C = \sigma_1^2$$
$$\Leftrightarrow p[C^T\Gamma^{-1}C - C^T\Gamma^{-1}C[1 + \Omega p]^{-1}C^T\Gamma^{-1}C] = \sigma_1^2$$
$$\Leftrightarrow \Omega p[\Omega p - \Omega p[1 + \Omega p]^{-1}\Omega p] = \Omega\sigma_1^2$$

Now consider the following substitutions: $\Omega p = \mu$

$$\Rightarrow \mu\left[\mu - \mu^2\frac{1}{1+\mu}\right] = \Omega\sigma_1^2$$
$$\Leftrightarrow \mu^2\left[1 - \frac{\mu}{1+\mu}\right] = \Omega\sigma_1^2$$
$$\Leftrightarrow \mu^2\frac{1}{1+\mu} = \Omega\sigma_1^2$$
$$\Leftrightarrow \mu^2 - \Omega\sigma_1^2\mu - \Omega\sigma_1^2 = 0$$

Only the positive solution to this second order equation is relevant in our case, hence:

$$\mu = \frac{\Omega\sigma_1^2}{2} + \sqrt[2]{\frac{\Omega^2\sigma_1^4}{4} + \Omega\sigma_1^2} = \frac{\Omega\sigma_1^2}{2}\left[1 + \sqrt[2]{1 + \frac{4}{\Omega\sigma_1^2}}\right] = \Omega p$$

In conclusion the calculations on previous page leads to the equation:

$$p = \frac{\sigma_1^2}{2}\left[1 + \sqrt[2]{1 + \frac{4}{\left(\frac{\sigma_1^2}{\sigma_{21}^2} + \frac{\sigma_1^2}{\sigma_{22}^2} + \cdots + \frac{\sigma_1^2}{\sigma_{2N}^2}\right)}}\right]$$

This is the solution to the DARE for a Kalman filter basing its estimate only on previous samples. A filter also using the latest measurement to form an estimate would according to [reference to Glad & Ljung] be described by the equation:

$$\tilde{P} = \left(1 - \tilde{K}C\right)^2 P + \tilde{K}R_2\tilde{K}^T$$
$$\tilde{K} = PC^T[CPC^T + R_2]^{-1}$$

The particular application investigated in this thesis is deemed to have a disturbance covariance much larger than the measurement noise. Thus it is suspected that a filter considering not only previous samples, but also the most recent, will outperform the alternative. In order for the two different implementations to be compared, $\tilde{P}$ must be calculated.

$$\tilde{K} = PC^T[CPC^T + R_2]^{-1} \Rightarrow \tilde{K}C = C^T[CC^T + \Gamma]^{-1}C$$
$$\Rightarrow \tilde{K}C = C^T[\Gamma^{-1} - \Gamma^{-1}C[1 + C^T\Gamma^{-1}C]^{-1}C^T\Gamma^{-1}]C$$
$$\Rightarrow \tilde{K}C = C^T\Gamma^{-1}C - C^T\Gamma^{-1}C[1 + C^T\Gamma^{-1}C]^{-1}C^T\Gamma^{-1}C$$
$$\Rightarrow \tilde{K}C = \Omega p - \Omega p[1 + \Omega p]^{-1}\Omega p$$
$$\Rightarrow \tilde{K}C = \Omega p\left[1 - \frac{\Omega p}{1 + \Omega p}\right]$$
$$\Rightarrow \tilde{K}C = \frac{\Omega p}{1 + \Omega p}$$

This equation helps in determining one of the two terms in $\tilde{P}$. The second term can be determined through the following:

$$\tilde{K}R_2\tilde{K}^T = C^T[CC^T + \Gamma]^{-1}p\Gamma[CC^T + \Gamma]^{-1}C$$
$$\Leftrightarrow \tilde{K}(p\Gamma)\tilde{K}^T = pC^T[CC^T + \Gamma]^{-1}\Gamma[CC^T + \Gamma]^{-1}C$$
$$= pC^T[\Gamma^{-1} - \Gamma^{-1}C[1 + C^T\Gamma^{-1}C]^{-1}C^T\Gamma^{-1}]\Gamma[\Gamma^{-1} - \Gamma^{-1}C[1 + C^T\Gamma^{-1}C]^{-1}C^T\Gamma^{-1}]C$$
$$= pC^T[I - \Gamma^{-1}C[1 + C^T\Gamma^{-1}C]^{-1}C^T][\Gamma^{-1} - \Gamma^{-1}C[1 + C^T\Gamma^{-1}C]^{-1}C^T\Gamma^{-1}]C$$
$$= pC^T[I - \Gamma^{-1}C[1 + \Omega p]^{-1}C^T][\Gamma^{-1} - \Gamma^{-1}C[1 + \Omega p]^{-1}C^T\Gamma^{-1}]C$$
$$= p\Omega p - \Omega p(1 + \Omega p)^{-1}\Omega p - \Omega p(1 + \Omega p)^{-1}\Omega p + p\Omega p(1 + \Omega p)^{-1}\Omega p(1 + \Omega p)^{-1}\Omega p$$
$$= \Omega p^2 - 2\Omega^2 p^3(1 + \Omega p)^{-1} + \Omega^3 p^4(1 + \Omega p)^{-2}$$
$$= \Omega p^2(1 - 2\Omega p(1 + \Omega p)^{-1} + \Omega^2 p^2(1 + \Omega p)^{-2})$$
$$= \Omega p^2\left(1 - \frac{\Omega p}{1 + \Omega p}\right)^2 = \frac{\Omega p^2}{(1 + \Omega p)^2}$$

In conclusion the calculations on the equations on the previous page can be used to form an expression for $\tilde{p}$:

$$\tilde{p} = \left(1 - \frac{\Omega p}{1 + \Omega p}\right)^2 p + \frac{\Omega p^2}{(1 + \Omega p)^2}$$

$$= \frac{p + \Omega p^2}{(1 + \Omega p)^2}$$
$$= \frac{p(1 + \Omega p)}{(1 + \Omega p)^2}$$

$$\Rightarrow \tilde{p} = \frac{p}{1 + \Omega p} < p$$

Given that both p and Ω are strictly positive, it becomes obvious that $\tilde{p} < p$. Since these two variables are the covariance of their respective Kalman filter implementations, this relationship dictates the expected conclusion that:
Sensor fusion implemented with a Kalman filter will always have better performance when including the latest sample in the estimate together with previous samples, instead of only using previous samples.
Assume that $\Omega = \sum_{i=1}^{N} \frac{1}{\sigma_{2i}^2} = \frac{1}{\sigma_2^2}$. Apparently an analogy can be drawn between using sensor fusion to decrease estimate variance and using parallel coupling of resistors to decrease resistance. Notice how this substitution affects p.

$$p = \frac{\sigma_1^2}{2}\left(1 + \sqrt[2]{1 + \frac{4\sigma_2^2}{\sigma_1^2}}\right) = \frac{\sigma_1^2}{2}(1 + \Psi)$$
$$\tilde{p} = \frac{\frac{\sigma_1^2}{2}(1 + \Psi)}{1 + \frac{\sigma_1^2}{2\sigma_2^2}(1 + \Psi)} = \frac{\sigma_1^2\sigma_2^2(1 + \Psi)}{2\sigma_2^2 + \sigma_1^2(1 + \Psi)}$$

$$\Rightarrow \frac{\tilde{p}}{p} = \frac{\sigma_1^2\sigma_2^2(1 + \Psi)}{2\sigma_2^2 + \sigma_1^2(1 + \Psi)} \cdot \frac{2}{\sigma_1^2(1 + \Psi)} = \frac{2\sigma_2^2}{2\sigma_2^2 + \sigma_1^2(1 + \Psi)} = \frac{2\sigma_2^2}{2\sigma_2^2 + \sigma_1^2\left(1 + \sqrt[2]{1 + \frac{4\sigma_2^2}{\sigma_1^2}}\right)}$$

As mentioned; it is assumed that for the particular application of this work the process disturbances are much greater than the measurement noise. Consider the above ratio for the case that $\sigma_1^2 \gg \sigma_2^2$:

$$\frac{\tilde{p}}{p} = \frac{2\sigma_2^2}{2\sigma_2^2 + \sigma_1^2\left(1 + \sqrt[2]{1 + \frac{4\sigma_2^2}{\sigma_1^2}}\right)} \approx \frac{1}{1 + \frac{\sigma_1^2}{2\sigma_2^2} + \frac{\sigma_1^2}{2\sigma_2^2}\left(1 + \frac{2\sigma_2^2}{\sigma_1^2}\right)} = \frac{1}{2 + \frac{\sigma_1^2}{\sigma_2^2}} = \frac{\sigma_2^2}{2\sigma_2^2 + \sigma_1^2}$$

Now assume that $\sigma_{2i}^2 = \lambda_2^2$ for all values of i, or in other words; all sensors have equal variance. That would mean that:

$$\sigma_2^2 = \frac{\lambda_2^2}{n} \Rightarrow \frac{\tilde{p}}{p} = \frac{\left(\frac{\lambda_2^2}{\sigma_1^2 n}\right)}{\left(1 + \frac{2}{n} \cdot \frac{\lambda_2^2}{\sigma_1^2}\right)}$$

With given assumptions complemented with the assumption of an increasing value of n, this expression will approach:

$$\frac{\tilde{p}}{p} = \frac{\lambda_2^2}{\sigma_1^2 n}$$